

A new moving strategy for the sequential Monte Carlo approach in optimizing the hydrological model parameters



Gaofeng Zhu^{a,*}, Xin Li^{b,c}, Jinzhu Ma^a, Yunquan Wang^d, Shaomin Liu^e, Chunlin Huang^b, Kun Zhang^a, Xiaoli Hu^b

^a Key Laboratory of Western China's Environmental Systems (Ministry of Education), Lanzhou University, Lanzhou 730000, China

^b Key Laboratory of Remote Sensing of Gansu Province, Cold and Arid Regions Environmental and Engineering Research Institute, Chinese Academy of Sciences, Lanzhou 730000, China

^c Chinese Academy of Sciences Center for Excellence in Tibetan Plateau Earth Sciences, Beijing 100101, China

^d School of Environmental Studies, China University of Geosciences, Wuhan, 430074, China

^e State Key Laboratory of Earth Surface Processes and Resource Ecology, Faculty of Geographical Science, Beijing Normal University, Beijing 100875, China

ARTICLE INFO

Article history:

Received 6 January 2017

Revised 6 February 2018

Accepted 7 February 2018

Available online 13 February 2018

Keywords:

Sequential Monte Carlo
Genetic algorithm

Bayes

Parameter optimization
Hydrologic models

MCMC

ABSTRACT

Sequential Monte Carlo (SMC) samplers have become increasingly popular for estimating the posterior parameter distribution with the non-linear dependency structures and multiple modes often present in hydrological models. However, the explorative capabilities and efficiency of the sampler depends strongly on the efficiency in the move step of SMC sampler. In this paper we presented a new SMC sampler entitled the Particle Evolution Metropolis Sequential Monte Carlo (PEM-SMC) algorithm, which is well suited to handle unknown static parameters of hydrologic model. The PEM-SMC sampler is inspired by the works of Liang and Wong (2001) and operates by incorporating the strengths of the genetic algorithm, differential evolution algorithm and Metropolis-Hastings algorithm into the framework of SMC. We also prove that the sampler admits the target distribution to be a stationary distribution. Two case studies including a multi-dimensional bimodal normal distribution and a conceptual rainfall-runoff hydrologic model by only considering parameter uncertainty and simultaneously considering parameter and input uncertainty show that PEM-SMC sampler is generally superior to other popular SMC algorithms in handling the high dimensional problems. The study also indicated that it may be important to account for model structural uncertainty by using multiplier different hydrological models in the SMC framework in future study.

© 2018 Elsevier Ltd. All rights reserved.

1. Introduction

Over the past few decades, considerable progress has been made in the development of hydrologic models, which are now widely used for different purposes such as flood forecasting, urban planning and water resources management (Pokhrel et al., 2008; Clark et al., 2015). It is well recognized that parameter estimation (model calibration) is a necessary step to improve model accuracy, and how to obtain appropriate model parameters has long been a subject of debate within the hydrologic community (Gupta et al., 1998; Montanari, 2005; Marshall et al., 2004; Montanari and Koutsoyiannis, 2012; Mendoza et al., 2015). Enabled by increasing computer power, tremendous advances have been achieved in parameter estimation methods (e.g., Duan et al., 1992; Gupta et al., 1998; Bates and Campbell, 2001; Vrugt et al., 2009; Pokhrel et al., 2012; Vrugt, 2016). Among them, Bayesian inference provides an

ideal platform for assessing parameter values by simultaneously accounting for both measurement and model structure uncertainties (Thiemann et al., 2001; Jeremiah et al., 2011; Gao and Zhang, 2012; Zhu et al., 2014), and is becoming increasingly popular in environment science (Clark, 2005).

Given the analytically intractable nature of the hydrologic models, implementation of Bayesian inference is usually aided by Markov chain Monte Carlo (MCMC) techniques (Smith and Marshall, 2008). In practice, the major difficulty associated with using MCMC is the need to assess convergence (Fan et al., 2008). Although there are several indices to help gauge convergence, for complex models one may never be completely sure (Clark, 2005). Sequential Monte Carlo (SMC) samplers (also known as particles filters) provide an alternative framework of drawing samples from the posterior distribution, which does not depend on Markov chain property, thereby avoiding the difficulty of ensuring chain convergence to the posterior distribution (Fan et al., 2008; Jeremiah et al., 2011). Traditionally, SMC samplers were developed primarily for estimation of the dynamic states in a system through various

* Corresponding author.

E-mail address: zhugf@lzu.edu.cn (G. Zhu).

reweighting, resampling and move strategies (Arulampalam et al., 2002). In hydrologic models, many (if not all) parameters that represent conceptual or effective properties of landscape should be regarded as time-invariant (static), and their meaningful values can only be obtained through the parameter-calibration method (Ajami et al., 2007; Mendoza et al., 2015). Now, several methods have been proposed to handle unknown static model parameters using the SMC samplers, including the state augmentation method, which simply treats the static parameters as dynamic states and transfer the parameter optimization to state-variable filtering problem (e.g., Moradkhani et al., 2005, 2012; Salamon and Feyen, 2009; Nagarajan et al., 2011; Noh et al., 2011; Vrugt et al., 2013; Abbaszadeh et al., 2018), and the dynamic partial posterior distribution method which sequentially incorporates increasing amounts of observations into the posterior distribution (e.g., Chopin, 2002). Another approach is the so-called geometric bridge method (Del Moral et al., 2006; Fan et al., 2008; Jeremiah et al., 2011, 2012), which constructs an inhomogeneous sequence of distributions to move smoothly from a tractable initial distribution to the target distribution through a sequence of intermediary distributions.

The SMC sampler implemented using geometric bridge method has advantages in preserving the static nature of the unknown parameters and inferring the parameter posterior distribution based on the whole observations (Lee and Chia, 2002). In spite of these advantages, the SMC sampler has a serious drawback, which is the well known *particle impoverishment* problem. To improve particle diversity and quality, the particles usually need to be moved by using the Markov Chain Monte Carlo (MCMC) transition kernel [i.e., random walk Metropolis (RWM) algorithm (Metropolis et al., 1953) and adaptive random walk Metropolis (ARM) algorithm (Chopin, 2002; Fan et al., 2008; Jeremiah et al., 2011, 2012)]. Chopin (2002) pointed out that the efficiency in the move step is critical since it is the most computationally demanding step. Thus, it is significantly important to develop appropriate candidate-generating algorithms in improving the efficiency of the SMC sampler (Owen and Tribble, 2005). Inspired by the success of the genetic and evolution algorithm (Holland, 1975; Storn and Price, 1997) in optimization problems, we proposed a new candidate-generating method in the framework of SMC by employing the two genetic-style operators (crossover and mutation). Specifically, the new algorithm is implemented by incorporating some attractive features of genetic and evolutionary algorithm to generate candidates as well as the Metropolis–Hastings algorithm into the framework of SMC to evolve the particles to the target distribution. This philosophy is not completely new. In previous studies, some authors have tried to combine the genetic or evolutionary algorithms with population MCMC (e.g., Liang and Wong, 2001; ter Braak, 2006; Vrugt et al., 2008). Also, considerable efforts have been paid to introduce the genetic algorithm into the particle filters (Uosaki et al., 2004; Park et al., 2007; Li et al., 2013; Abbaszadeh et al., 2018). However, these works mainly focus on estimating the state variables of a dynamic system rather than the unknown model parameters. In this study, we describe how to embed the genetic and evolutionary algorithm into the framework of SMC for estimating the static model parameters, and prove that the proposed algorithm in move step is an MCMC transition kernel which admits the intermediary distribution to be stationary. In addition, there is a growing realization that parameter estimation in hydrological models is significantly affected by uncertainties in the input-forcing data (Kavetski et al., 2002, 2006; Ajami et al., 2007; Vrugt et al., 2008). To get unbiased parameter estimations and detect the genuine model structure inadequacies, the forcing uncertainty should be described explicitly with the system through input error models (Kavetski et al., 2002, 2006; Ajami et al., 2007; Vrugt et al., 2008). In such conditions, the number of variables needed to be estimated (including hydrological model parameters

and “latent variables” in the input error model) increase considerably and often cause dimensionality issues (Ajami et al., 2007). Thus, it is needed for the SMC samplers to be able to handle the high dimensional problems, and the applicability of the samplers for analyzing forcing uncertainty should be assessed systematically (Montanari, 2007). To achieve this propose, the efficiency and effectiveness of the proposed SMC sampler were tested and compared with other SMC samplers using different MCMC transitional kernels (i.e., RWM and ARW algorithms) through two case studies. The first one uses a synthetic bimodal normal distribution with dimensions varying from 5 to 50, and the second one uses a conceptual rainfall-runoff model by dealing only with model parameter uncertainty and simultaneously with model parameter and input uncertainties.

The paper is organized as follows. Section 2 presents a summary of the Bayesian inference, followed by a detailed description of the SMC samplers in Section 3, including the principle of the geometric bridge method, the procedures of the SMC sampler, and the candidate generating methods in move step. Section 4 provides the results of the two case studies and compares the performance of each sampler. Finally, Section 5 presents the main conclusions of the study and the scope for future work.

2. Bayesian inference

A hydrological model can be defined as:

$$\bar{y}_t = f(\bar{x}_t; \theta) + \varepsilon_t \quad (1)$$

where \bar{y}_t is the observed data at time $t = \{1, 2, \dots, n\}$; $f(\bar{x}_t; \theta)$ is the corresponding model output (simulation); \bar{x}_t is the model input at time t ; $\theta \in R^d$ is a d -dimensional vector of unknown model parameters; and ε_t represents the measurement error, consisting the combined errors from modeling uncertainties.

The Bayesian inference treats hydrologic model parameters, θ , as probabilistic variables, and the posterior parameter distributions can be expressed as:

$$p(\theta | \bar{y}_{1:n}) = \frac{p(\theta)p(\bar{y}_{1:n}|\theta)}{p(\bar{y}_{1:n})} \propto p(\theta)p(\bar{y}_{1:n}|\theta) \quad (2)$$

where $\bar{y}_{1:n} = \{\bar{y}_t; t = 1, 2, \dots, n\}$ represents the set of all available observations; $p(\theta)$ and $p(\theta|\bar{y}_{1:n})$ signify the prior and posterior parameter distribution, respectively; $p(\bar{y}_{1:n}|\theta)$ denotes the model likelihood for observed data $\bar{y}_{1:n}$; and $p(\bar{y}_{1:n})$ is the normalization constant so that the posterior parameter distribution integrates to unity. In the most simplistic case with scalar valued measurement ($\bar{y}_t \in R^1; t = 1, 2, \dots, n$) and normal homoscedastic, uncorrelated error terms, the likelihood function can be written as:

$$p(\bar{y}_{1:n}|\theta) = (2\pi\sigma^2)^{-n/2} \prod_{t=1}^n \exp \left\{ -\frac{[\bar{y}_t - f(\bar{x}_t; \theta)]^2}{2\sigma^2} \right\} \quad (3)$$

where σ is an estimate of the standard deviation of the measurement error. Traditionally, σ can be included into the analysis explicitly (i.e., assuming σ is uniform over $\log \sigma$; Gelman et al., 1995; Bates and Campbell, 2001) and treated as one the model parameters, which yields a complete posterior distribution of σ . However, this method artificially increased the parameter dimension of the problem and may result in unreasonable estimations of the parameter values (Kavetski et al., 2006). In this study, σ was estimated by using the analytical method (Braswell et al., 2005; Zhu et al., 2014), which is to find the value of σ that maximizes $\log[p(\bar{y}_{1:n}|\theta)]$ for a given parameter vector. By differentiating $\log[p(\bar{y}_{1:n}|\theta)]$ with respect to σ , we can obtain:

$$\sigma_a = \sqrt{\frac{1}{n} \sum_{t=1}^n [\bar{y}_t - f(\bar{x}_t; \theta)]^2} \quad (4)$$

We then used σ_a to replace σ in Eq. (3).

3. Sequential Monte Carlo sampling

The sequential Monte Carlo (SMC) sampling approach is a generalization of importance sampling that generates a set of samples from $p(\theta|\bar{y}_{1:n})$ with associated weights (also called *particles*) and calculates estimates based on these weighted samples. As the number of samples become very large, the Monte Carlo approximation can equivalently represent the functional description of the posterior distribution (Arulampalam et al., 2002). However, since the posterior distribution is hard to sample directly, SMC tackles this problem by introducing a sequence of intermediary distributions with the final distribution given by the desired posterior (Fan et al., 2008). In this study, the intermediary distribution is constructed using the geometric bridge method (Del Moral et al., 2006; Fan et al., 2008; Jeremiah et al., 2011,2012):

$$\pi_s(\theta) \propto p_0(\theta)^{1-\beta_s} p(\theta|\bar{y}_{1:n})^{\beta_s} \quad (5)$$

where $p_0(\theta)$ and $\pi_s(\theta)$ denote the initial and the s th distribution in the sequence ($s=0, 1, \dots, S$), respectively; and $\{\beta_s\}$ is a sequence of scalar powers such that $0 \leq \beta_0 \leq \beta_1 \leq \dots \leq \beta_S = 1$, which allows a gradual transition of $\pi_s(\theta)$ from the initial sampling distribution, $\pi_0(\theta) \propto p_0(\theta)$, when $\beta_0 = 0$, to the posterior distribution, $\pi_S(\theta) \propto p(\theta|\bar{y}_{1:n})$, when $\beta_S = 1$. How to specify the distributional sequence $\{\beta_s\}$ still remains an open research question (Fan et al., 2008). Following Jeremiah et al. (2011, 2012), an exponential $\{\beta_s\}$ sequence is used in this study.

Suppose that an initial population of N particles (i.e. parameter vectors θ) are generated from the initial distribution $\pi_0(\theta) \propto p_0(\theta)$, from which direct sampling is possible. Each particle is denoted by θ_j^0 and allocated a weight $w_j^0 \equiv 1/N$ for $j = 1, 2, \dots, N$, so that $\{\theta_j^0, w_j^0\}$ is a weighted particle at initial stage $s=0$. The SMC sampling approach then uses the weighted particles from $\pi_{s-1}(\theta)$ (with $s=1, 2, \dots, S$) to produce particles from distribution $\pi_s(\theta)$ through reweighting, resampling and move processes, which are described in detail below.

3.1. Reweighting

Given N weighted particles $\{\theta_j^{s-1}, w_j^{s-1}\}$ ($j=1, 2, \dots, N$) from $\pi_{s-1}(\theta)$ at stage $s-1$ (with $s=1, 2, \dots, S$), then by setting $\theta_j^s = \theta_j^{s-1}$, and

$$w_j^s = w_j^{s-1} \frac{\pi_s(\theta_j^s)}{\pi_{s-1}(\theta_j^{s-1})} \quad (6)$$

The resulting particles, $\{\theta_j^s, w_j^s\}$, are now drawn from the distribution $\pi_s(\theta)$. Eq. (6) will increase the weight of particles that have higher density under $\pi_s(\theta)$ than under $\pi_{s-1}(\theta)$, and decrease the weight of particles that have lower density under $\pi_s(\theta)$ than under $\pi_{s-1}(\theta)$.

3.2. Resampling

A common problem with the SMC sampling approach is the degeneracy phenomenon, where as s increases, all but one particle will have negligible weight (Arulampalam et al., 2002). This implies that a large computational effort is devoted to updating particles whose contribution to posterior estimates and predictions is almost zero. The aim of resampling step is to discard “bad” particles with negligible importance and to replace them with exact copies of more promising samples (Vrugt et al., 2013). A suitable measure of degeneracy of the algorithm is the effective sample size

(N_{eff}), defined as (Jeremiah et al., 2011,2012; Vrugt et al., 2013):

$$N_{eff} = \frac{1}{\sum_{i=1}^N (w_i^s)^2} \quad (7)$$

In practice, resampling is performed whenever N_{eff} is less than rN , where $r \in [0, 1]$ is a pre-specified constant typically taken to be 1/2 (Fan et al., 2008). The resulting particle is in fact an *i.i.d* sample from the discrete distribution $\{\theta_j^s, w_j^s\}$ (Arulampalam et al., 2002), and the weights are reset to $w_j^s = 1/N$ for $j = 1, 2, \dots, N$ (Fan et al., 2008; Jeremiah et al., 2011,2012). Until now, a wide-variety of resampling methods including systematic, stratified, residual and multinomial resampling has been developed in the statistical literature. Following Arulampalam et al. (2002), the systematic resampling scheme is selected in this study since it is simple to implement and minimizes the Monte Carlo variance.

3.3. Move

Although the resampling step reduces the effects of the degeneracy problem, it may lead to a loss of diversity among the particles as the resulting sample will contain many repeated points, which is known as *sample impoverishment*. Let $\{\theta_j^s, w_j^s\}$ ($j=1, 2, \dots, N$) denote particles at current stage s after reweighting and (possibly) resampling steps. To improve particle diversity and quality, each sample is moved according to a Markov Chain Monte Carlo (MCMC) transition kernel, K_s , so that $\bar{\theta}_j^s \sim K_s(\theta_j^s, \cdot)$. Generally, the building of a MCMC transition kernel K_s proceeds in the following three steps. First, a candidate particle $\bar{\theta}_j^s$ is sampled from a proposal density $q_s(\cdot|\theta_j^s)$ that depends on the present particle, θ_j^s . Next, the candidate particle is either accepted or rejected using the Metropolis–Hastings (M–H) acceptance probability:

$$\alpha = \min \left\{ 1, \frac{\pi_s(\bar{\theta}_j^s) q_s(\theta_j^s | \bar{\theta}_j^s)}{\pi_s(\theta_j^s) q_s(\bar{\theta}_j^s | \theta_j^s)} \right\} \quad (8)$$

Finally, with probability α set $\theta_j^s = \bar{\theta}_j^s$, else leave θ_j^s unchanged.

Efficiency of the move step significantly depends on an appropriate selection of the candidate-generating methods (Owen and Tribble, 2005). The earliest and most general candidate-generating approach is the random walk Metropolis (RWM) algorithm (Metropolis et al., 1953). In this approach, the candidate sample $\bar{\theta}_j^s$ is drawn from a proposal density $q_s(\cdot|\bullet)$ that depends on the current particle, θ_j^s and is assumed to be fixed and symmetric (i.e., $q_s(\bar{\theta}_j^s|\theta_j^s) = q_s(\theta_j^s|\bar{\theta}_j^s)$). A natural choice for $q_s(\cdot|\theta_j^s)$ in practice is the multivariate normal density, so that $\bar{\theta}_j^s \sim N_d(\theta_j^s, \gamma \mathbf{I}_d)$. Here, \mathbf{I}_d denotes the d -dimensional identity matrix, and γ is the scaling factor for which we have used the value $\gamma = 2.38/\sqrt{2d}$ given by Roberts and Rosenthal (1998). To fully use the information gained by the particle system itself, the adaptive random walk Metropolis (ARM) algorithm is proposed and has been widely used in literature (Chopin, 2002; Fan et al., 2008; Jeremiah et al., 2011,2012). For the ARM algorithm, the covariance of the multivariate normal proposal density is continuously adapted toward the target distribution based on particles in previous populations. Following Chopin (2002), the proposal density is defined as $q_s(\cdot|\theta_j^s) = N_d(\theta_j^s, \Sigma_{s-1})$, where Σ_{s-1} denotes the weighted sample covariance matrix of previous particle populations, $\{\theta_j^{s-1}, w_j^{s-1}\}$, ($j=1, 2, \dots, N$).

The new candidate-generating method presented here is named as Particle Evolution Metropolis (PEM), which uses genetic and evolution operators to generate candidates (Holland, 1975; Storn and Price, 1997), and merges the strength of the M–H algorithm

to evolve the particle to the target distribution. In the context of genetic or evolution algorithm, the particle ($\theta_j^s, j=1, 2, \dots, N$) at current stage s is called a *chromosome* or an *individual*, and the set of N particles form a population. Then, the population is continuously updated toward better solutions in the parameter space by selection and modification procedures. Noticeably, the particles have been selected according to their weights in the resampling step of the SMC algorithm, which is functionally similar to the roulette wheel selection procedure used in genetic algorithm. Thus, only two genetic-styled operators, *crossover* and *mutation*, are employed in this step, and they serve to diversify the individuals in the population. Notably, the chromosomes can be coded as either binary or real numbers. In applications to practical problems, previous studies have demonstrated that the genetic-styled operators are more efficient for real-coded chromosomes than those coded in binary numbers (Liang and Wong, 2001). Thus, the real-coded chromosomes were used in this study.

In the crossover operator, one parental chromosome pair, θ_i^s and θ_j^s ($i \neq j$), is selected from the current population without replacement and mated to produce a new offspring pair, $\bar{\theta}_i^s$ and $\bar{\theta}_j^s$ according to the random selection procedure as the weights of chromosome were reset to be equal after the resampling step. Here, the simple one-point crossover operator is used to generate offspring ($\bar{\theta}_i^s$ and $\bar{\theta}_j^s$), which is operated as follows. First, an integer crossover point is drawn uniformly on $\{1, 2, \dots, d\}$ (where d is the dimension of parameter space); then $\bar{\theta}_i^s$ and $\bar{\theta}_j^s$ are produced by swapping the parameters to the right of the crossover point between parents (θ_i^s and θ_j^s) with a predefined crossover probability P_c . After crossover, the new offspring pair is accepted with probability $\min\{1, r_c\}$ according to the M-H rule:

$$r_c = \frac{\pi_s(\bar{\theta}_i^s)\pi_s(\bar{\theta}_j^s)J_s((\theta_i^s, \theta_j^s)|(\bar{\theta}_i^s, \bar{\theta}_j^s))}{\pi_s(\theta_i^s)\pi_s(\theta_j^s)J_s((\bar{\theta}_i^s, \bar{\theta}_j^s)|(\theta_i^s, \theta_j^s))} \quad (9)$$

where $J_s(\bullet|\bullet)$ denotes the transfer probability between the parental (θ_i^s, θ_j^s) and the offspring ($\bar{\theta}_i^s, \bar{\theta}_j^s$) pairs, and $J_s((\bar{\theta}_i^s, \bar{\theta}_j^s)|(\theta_i^s, \theta_j^s)) = P((\theta_i^s, \theta_j^s)|\Theta) \times P((\bar{\theta}_i^s, \bar{\theta}_j^s)|(\theta_i^s, \theta_j^s))$. Here, $P((\theta_i^s, \theta_j^s)|\Theta)$ denotes the selection probability of one pair from the parental population Θ , and $P((\bar{\theta}_i^s, \bar{\theta}_j^s)|(\theta_i^s, \theta_j^s))$ is the generating probability of offspring pair ($\bar{\theta}_i^s, \bar{\theta}_j^s$) from the parental chair (θ_i^s, θ_j^s). It can be proved that the transfer probability from the parental pair (θ_i^s, θ_j^s) to the offspring pair ($\bar{\theta}_i^s, \bar{\theta}_j^s$) is equal to the reverse transfer, i.e., $J_s((\bar{\theta}_i^s, \bar{\theta}_j^s)|(\theta_i^s, \theta_j^s)) = J_s((\theta_i^s, \theta_j^s)|(\bar{\theta}_i^s, \bar{\theta}_j^s))$ (see theorem in **Supplement 1**). If the proposal is accepted, the current parental pair (θ_i^s, θ_j^s) in the population is replaced by ($\bar{\theta}_i^s, \bar{\theta}_j^s$), otherwise the population remains unchanged. Noticeably, if mating does not take place in the crossover procedure, the parents always survive to the next stage according to the M-H rule. After the crossover operators (which repeat $N/2$ times), the population is updated and denoted by $\Theta = \{\theta_j^s, j=1, 2, \dots, N\}$.

To increase the diversity of the parameter population, the differential mutation procedure is used to modify the real-coded chromosomes of offspring (Storn and Price, 1997). That is, the current particle, θ_j^s ($j=1, 2, \dots, N$), is mutated according to:

$$\bar{\theta}_j^s = \theta_j^s + \gamma(\theta_{r_1}^s - \theta_{r_2}^s) + \zeta_d \quad (10)$$

where r_1 and r_2 are integer values drawn without replacement from $\{1, \dots, j-1, j+1, \dots, N\}$; $\gamma = 2.38/\sqrt{2d}$ denotes the jump rate; and $\zeta_d \sim N_d(0, b^*)$ is drawn from a normal density with small standard deviation, say $b^* = 10^{-6}$. According to the M-H rule, the new chromosome $\bar{\theta}_j^s$ is accepted with probability $\min\{1, r_m\}$, where r_m

is calculated as:

$$r_m = \frac{\pi_s(\bar{\theta}_j^s)J_s(\theta_j^s|\bar{\theta}_j^s)}{\pi_s(\theta_j^s)J_s(\bar{\theta}_j^s|\theta_j^s)} \quad (11)$$

and $J_s(\bullet|\bullet)$ denotes the transition probability between θ_j^s and $\bar{\theta}_j^s$. ter Braak (2006) has proved that the transfer probability from $\bar{\theta}_j^s$ to θ_j^s is the same as that from θ_j^s to $\bar{\theta}_j^s$, i.e., $J_s(\bar{\theta}_j^s|\theta_j^s) = J_s(\theta_j^s|\bar{\theta}_j^s)$. If the proposal is accepted, the current parental chromosome θ_j^s in the population is replaced by $\bar{\theta}_j^s$, otherwise the population remains unchanged. These operators (selection and mutation) are repeated N times and the population is updated again.

We proved that the PEM algorithm maintains the detailed balance and admits $\pi_s(\bullet)$ as the unique stationary distribution at each stage s (see theorem in **Supplement 1**). There are only three basic control variables in PEM-SMC sampler: N , the number of particles in population, S , the number of evolutions and P_c , the crossover probability (which is set to be 0.6 in this study). In addition, it is inherently parallel and hence lends itself to computation via a parallel machine or a network of computers. The pseudo-code of the algorithm is given below.

STEP 1: Initialization:

- (a) Draw an initial population $\{\theta_j^0\}$ ($j=1, 2, \dots, N$) from $p_0(\theta)$, and set weights $w_j^0 = 1/N$.
- (b) Identify the sequence $0 \leq \beta_0 \leq \beta_1 \leq \dots \leq \beta_S = 1$.
- (c) Set iteration index $s=1$, and effective sample size constant, $r \in [0, 1]$.

FOR $s \leftarrow 1, 2, \dots, S$ DO (Stage Evolution)

STEP 2: Reweighting:

- (a) Set $\theta_j^s = \theta_j^{s-1}$ ($j=1, \dots, N$), and calculate the weight, $w_j^s = w_j^{s-1} \frac{\pi_s(\theta_j^s)}{\pi_{s-1}(\theta_j^{s-1})}$.
- (b) Normalize the weight so that $\sum_{j=1}^N w_j^s = 1$.

STEP 3: Resampling?

- (a) Calculate the effective sample size, $N_{eff} = 1 / \sum_{i=1}^N (w_j^s)^2$.
- (b) If $N_{eff} < rN$, go to the next step; otherwise return to **STEP 2**

STEP 3A: Systematic resampling

- (a) Resample from $\{\theta_j^s, w_j^s\}$ ($j=1, 2, \dots, N$) using the systematic resampling procedure.
- (b) Set $w_j^s = 1/N$ ($j=1, 2, \dots, N$).

STEP 3B: Move using the PEM algorithm to increase the diversity of particles

FOR $i \leftarrow 1, 2, \dots, N/2$ DO (crossover operator using one pair chromosome)

- (a) Randomly select one parental chromosome pair, θ_i^s and θ_j^s ($i \neq j$), and create a new offspring pair, $\bar{\theta}_i^s$ and $\bar{\theta}_j^s$ using the one-point crossover operator.
- (b) With probability $\min\{1, \frac{\pi_s(\bar{\theta}_i^s)\pi_s(\bar{\theta}_j^s)J_s((\theta_i^s, \theta_j^s)|(\bar{\theta}_i^s, \bar{\theta}_j^s))}{\pi_s(\theta_i^s)\pi_s(\theta_j^s)J_s((\bar{\theta}_i^s, \bar{\theta}_j^s)|(\theta_i^s, \theta_j^s))}\}$, set $\theta_i^s = \bar{\theta}_i^s$ and $\theta_j^s = \bar{\theta}_j^s$, else leave θ_i^s and θ_j^s unchanged.

END FOR (Crossover Operator Using One Pair Chromosome)

FOR $i \leftarrow 1, 2, \dots, N$ DO (Mutation Operator Using One Chromosome)

- (a) Uniformly select one chromosome, θ_j^s ($j=1, 2, \dots, N$) from the present population, and create a new chromosome $\bar{\theta}_j^s$ by the mutation operator.

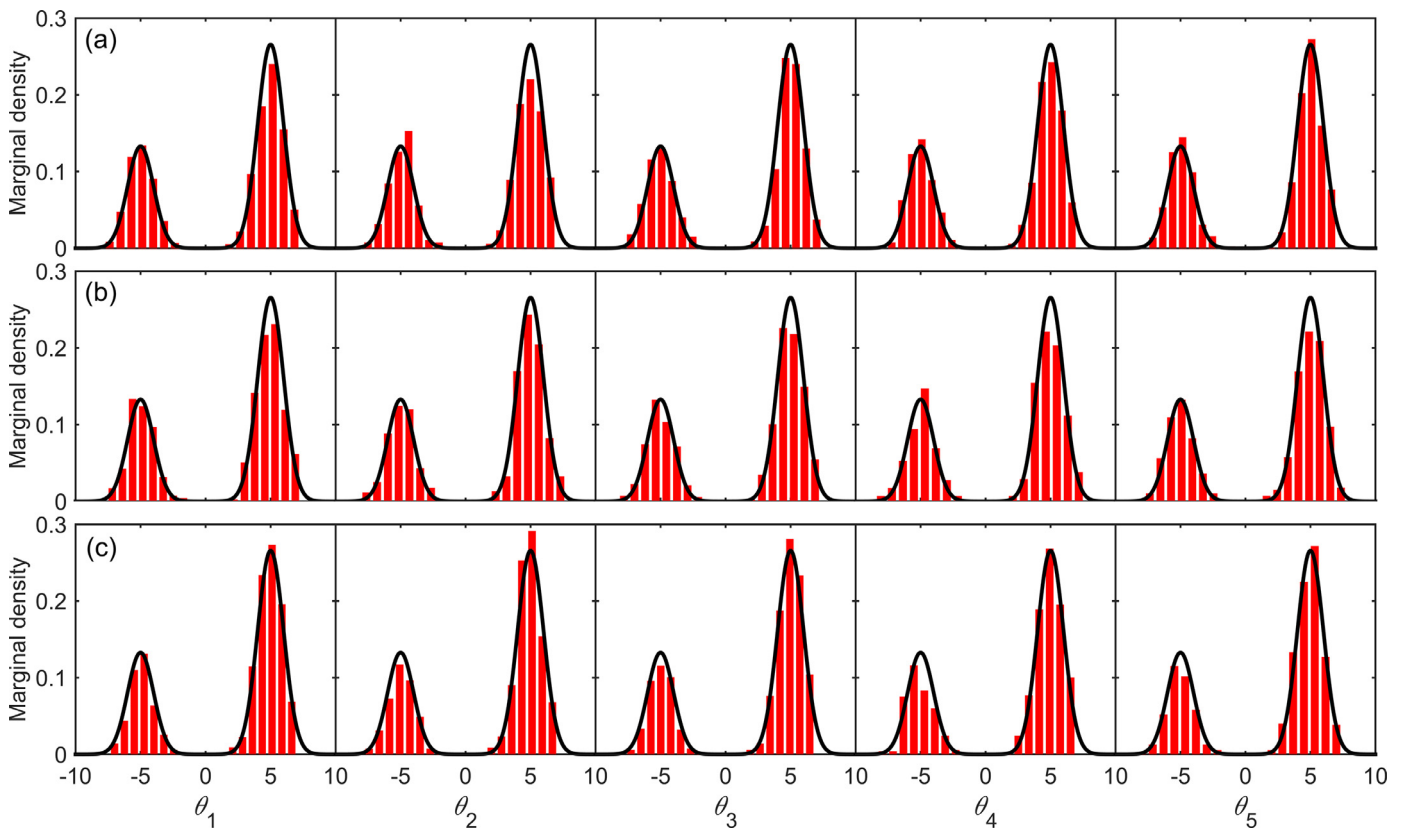


Fig. 1. The posterior marginal distribution of the 5-dimension bimodal normal distribution derived by (a) RWM-SMC, (b) ARM-SMC and (c) PEM-SMC samplers. The solid black line depicts the target distribution.

Table 1

Statistical properties about the average Euclidean distance of the SMC samplers estimated mean values and standard deviations from the true values over 100 independent runs for the bimodal normal distribution.

Dimension	RWM-SMC		ARM-SMC		PEM-SMC	
	Mean($\ E\ $)	SD($\ E\ $)	Mean($\ E\ $)	SD($\ E\ $)	Mean($\ E\ $)	SD($\ E\ $)
$d=5$	0.53	0.41	0.45	0.51	0.46	0.43
$d=10$	1.14	3.28	1.12	3.31	1.06	1.21
$d=20$	1.87	5.09	29.7	20.1	1.68	3.08
$d=30$	4.01	72.5	N/A	N/A	3.54	8.67

Mean($\|E\|$) denotes the average Euclidean distance of the SMC samples derived posterior mean values from their true values; thus Mean($\|E\|$) = $[\sum_{i=1}^d (\hat{\theta}_i - \theta_i)^2]^{1/2}$, where $\hat{\theta}_i$ and θ_i is the estimated and true parameter value in the i th dimension, respectively. Similarly, SD($\|E\|$) denotes the average Euclidean distance of the SMC samples derived standard deviations from their true values. To reduce the influence of sampling variability, the presented statistics denote over 100 independent runs.

(b) With probability $\min\{1, \frac{\pi_s(\bar{\theta}_j^s)J_s(\theta_j^s|\bar{\theta}_j^s)}{\pi_s(\theta_j^s)J_s(\bar{\theta}_j^s|\theta_j^s)}\}$, set $\theta_j^s = \bar{\theta}_j^s$, else leave θ_j^s unchanged.
END FOR (Mutation Operator Using One Chromosome)
END FOR (Stage Evolution)

conceptual rainfall-runoff watershed model with data from the Bass River watershed, Australia.

4.1. Case study 1: synthetic bimodal normal mixture

To emulate the common feature of the parameter surface with multiple modes in hydrological modeling, the first case study involves a synthetic multi-dimensional bimodal normal distribution (Smith and Marshall, 2008; Vrugt et al., 2009):

$$\pi(\theta) = \frac{1}{3}N_d(\theta; -\mathbf{5}, \mathbf{I}_d) + \frac{2}{3}N_d(\theta; \mathbf{5}, \mathbf{I}_d) \quad (12)$$

where $-\mathbf{5}$ and $\mathbf{5}$ are d -dimensional vectors. To explore the efficiency and effectiveness of the SMC samplers in simulating the target distribution in different dimensions, the test study was performed in dimensions $d=5, 10, 20$ and 30 . The feasible parameter space was taken to be a uniform distribution between -10 and 10 for each parameter.

In the 5-dimensional case, Fig. 1 compares histograms of the marginal posterior distribution of parameter derived from the SMC

4. Case studies

In this section, we conducted two case studies to compare the performance of the SMC sampler with different candidate-generating algorithms in exploring the parameter space. For convenience, the SMC sampler utilizing the RWM, ARM and PEM algorithms to generate candidates is named as RWM-SMC, ARM-SMC and PEM-SMC, respectively. In the first case study, a synthetic example is constructed on the basis of a mixture of multivariate normal distribution with a well-separated bimodal response surface. The second example considers application of the algorithms to parameter inference in the hydrologic setting, featuring a lumped

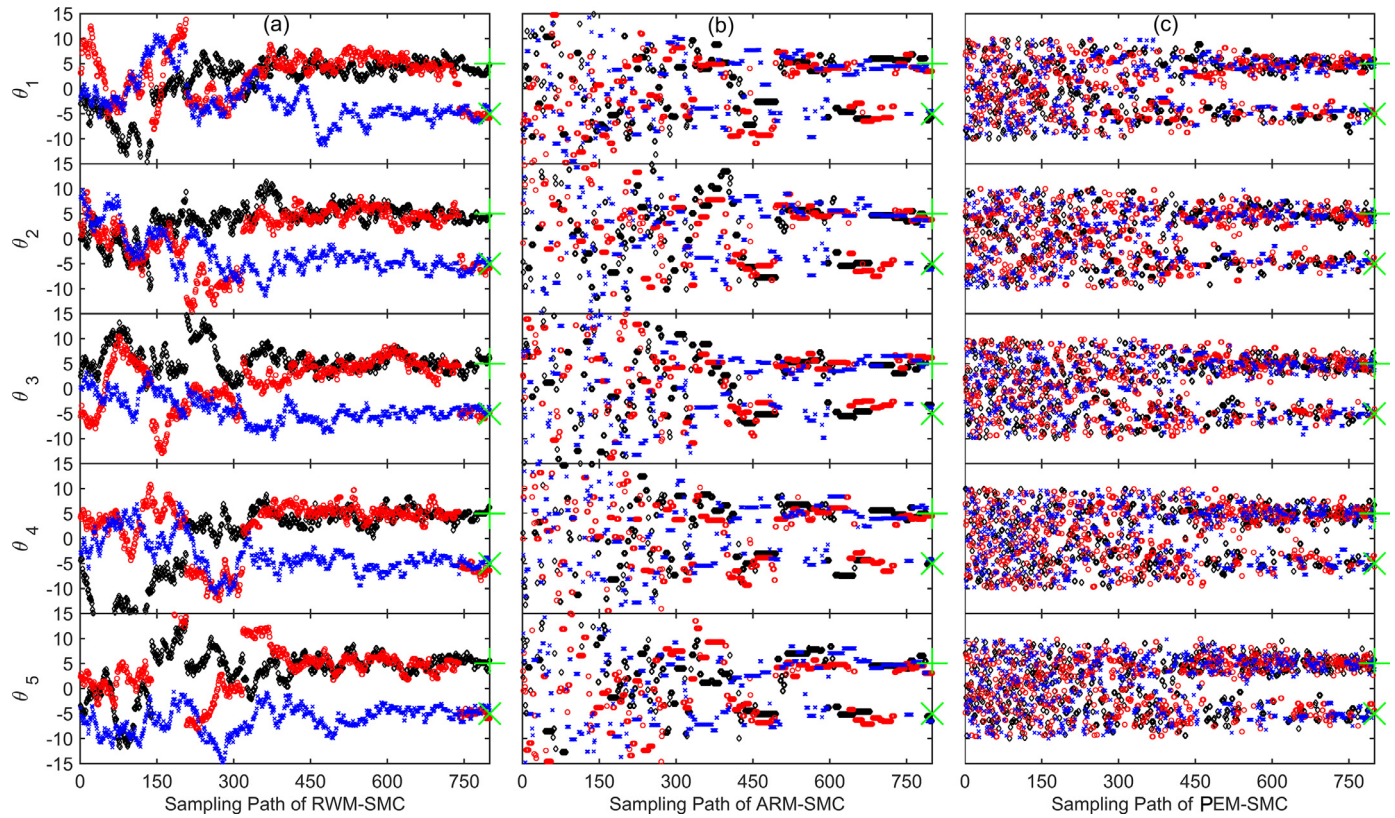


Fig. 2. Transitions of the parameters in 3 selected particles during the sampling path to the 5-dimension bimodal normal posterior target distribution using (a) RWM-SMC, (b) ARM-SMC and (c) PEM-SMC samplers. The actual target parameter values -5 and $+5$ are represented by ' \times ' and ' $+$ ' at the right hand side, respectively. For more explanation, please refer to the text. Different particle is coded with a different symbol and color.

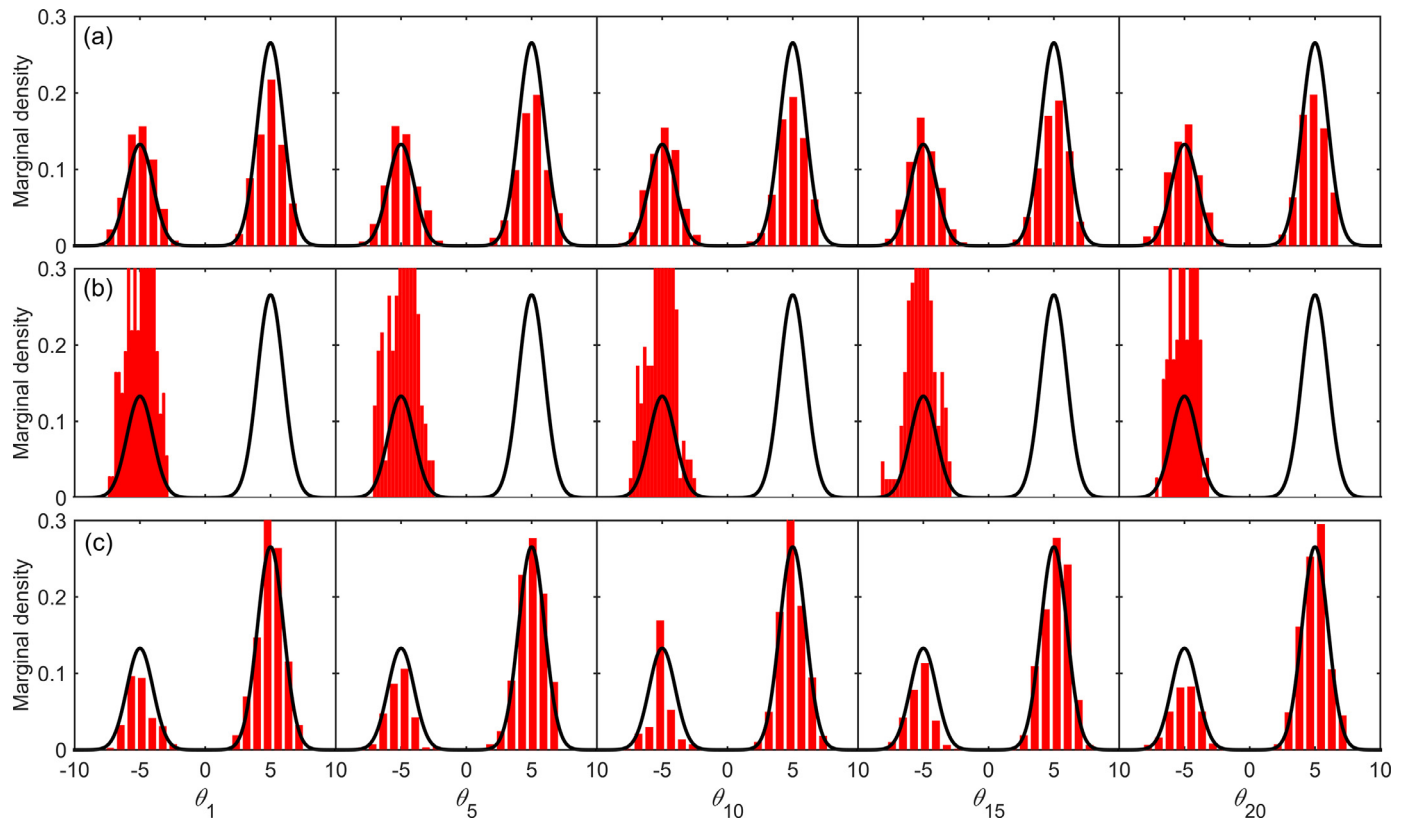


Fig. 3. The posterior marginal distribution of dimensions $\{1, 5, 10, 15, 20\}$ of the 20-dimension bimodal normal distribution generated by (a) RWM-SMC, (b) ARM-SMC and (c) PEM-SMC samplers. The solid black line depicts the target distribution.

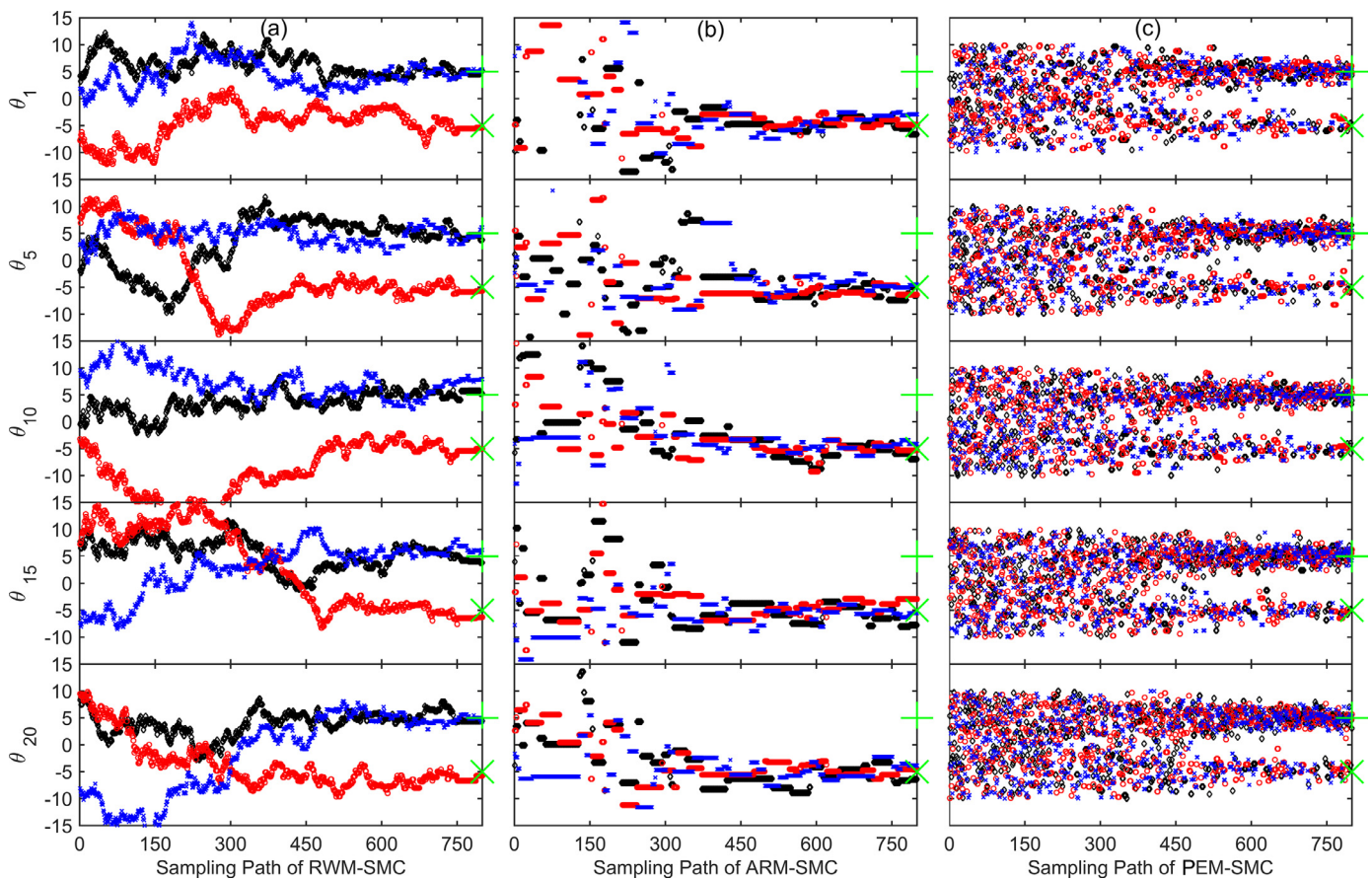


Fig. 4. Transitions of the sampled parameters of dimensions $\{1, 5, 10, 15, 20\}$ in 3 randomly selected particles during the sampling path using (a) RWM-SMC, (b) ARM-SMC and (c) PEM-SMC samplers. The actual target parameter values -5 and $+5$ are represented by 'x' and '+' at the right hand side, respectively. For more explanation, please refer to the text. Different particle is coded with a different symbol and color.

samplers with the actual target distribution. Obviously, both modes of the target distribution are well identified by the three SMC samplers (with particle number $N=300$). In addition, the statistical characteristics of the average Euclidean distance of the true means and standard deviations of the prior defined probability distribution from the respective values estimated with the SMC samplers are summarized in Table 1. The results indicated that the SMC samplers can give a reasonable estimation of the true values of the prior defined probability distribution. To check the convergence status of the SMC algorithms, the transitions of parameters of the selected particles during the sampling paths are illustrated in Fig. 2. Note, graphical examination about the convergences of the algorithms for other particles yields a similar picture as that presented in Fig. 2. It demonstrates that in the initial stages ($s < 450$), the parameter values of the particles are uniformly distributed in the parameter space. At a later stage ($s > 450$), they all tend to converge to a limiting distribution that appear relative tight and encompass the actual target parameter values (-5 and $+5$, represented by 'x' and '+' at the right hand side, respectively). However, the mixing of the particles generated by the RWM-SMC algorithm is quite poor. It is generally difficult for the particles to jump from one mode to the other, and the individual particle tends to collapse into a single region of highest attraction (Fig. 2a). On the contrary, the other two SMC samplers (i.e., ARM-SMC and PEM-SMC) exhibit relatively good explorative and mixing capabilities partially due to their abilities in exchanging information about the search space gained by different launched particles (Fig. 2b and c). The performances of the SMC samplers in dimension $d=10$ are similar to that in $d=5$. To obtain proper estimations of posterior

parameter distribution, the particle number should be larger than 800.

For the 20-dimensional case, the histograms of the marginal posterior distribution of dimensions $\{1, 5, 10, 15, 20\}$ generated using the SMC samplers (with particle number $N=1500$) are presented in Fig. 3, as well as providing the actual target distribution (black line). It is clear that the ARM-SMC sampler falsely converged to local optimum, and only one mode was identified by it. Also, the average Euclidean distance of the PEM-SMC estimated mean values and standard deviations from the true values is closer to zero than that of the other SMC samples, suggesting that the PEM-SMC sampler outperforms other SMC samplers in estimating the 20-dimensional bimodal target distribution. More significantly, the transitions of parameters during the sampling paths revealed that the particles generated by the RWM-SMC and ARM-SMC samplers tend to collapse into local optima, and the mixing of the particles are quite poor (Fig. 4a and b). On the contrary, the PEM-SMC algorithm exhibits relatively good mixing capabilities and thus maintaining the diversity of the particles (Fig. 4c). We further tested the performances of the SMC samplers in dimension $d=30$ with particle number $N=1500$. The results indicated that it is difficult for the RWM-SMC, and ARM-SMC samplers to properly estimate the 30-dimensional bimodal target distribution. In contrast, the PEM-SMC sampler illustrated relative good performances in both properly identifying two modes of the target distribution and maintaining the mixing properties of particles (see details in Supplement 2).

Thus, the PEM-SMC sampler seems to be more efficient in exploring the high dimensional and complex parameter space than

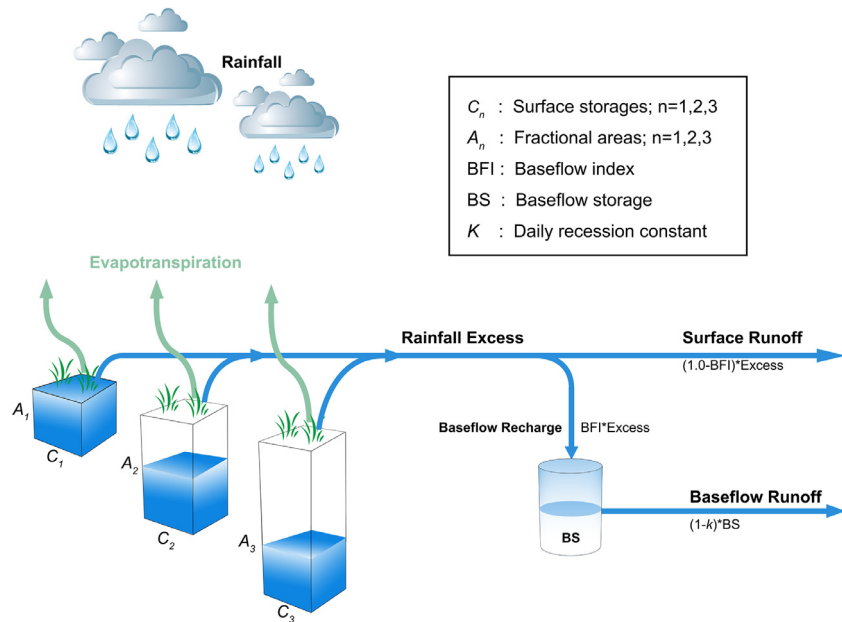


Fig. 5. Structure of the AWBM (modified according to Boughton, 1993).

other SMC-samplers (i.e., RWM-SMC and ARM-SMC). This does benefit from the ability of the genetic algorithm to learn efficiently from the historical evolutionary processes, which plays an important role in the early stage of the evolution. That is, the good particles (with a high probability value) tend to be stored in the population for a relative long time, while the bad particles (with a low probability value) will be easily eliminated from the population. Thus, the crossover operator in subsequent evolutionary processes ensures us to construct better proposal distributions based on the guidance of good particles stored in the population. In addition, the mutation operator provides a local updating step to help the particles escape from local optimum and therefore increase the mixing of the particles. The improved efficiency and effectiveness of the PEM-SMC algorithm give us confidence in its proper assessment of parameter uncertainty in hydrologic modeling.

4.2. Case study 2: conceptual hydrologic modeling

The second case study considers the Australian Water Balance Model (AWBM), which was developed by Boughton (1993) to calculate daily runoff from daily rainfall data and daily evapotranspiration estimates (Fig. 5). The AWBM has 8 parameters that need to be properly calibrated. Among them, six parameters represent the variability of soil moisture capacity over a watershed, which include three surface storage capacities (C_1 , C_2 , C_3) and the fractional areas associated with these capacities (A_1 , A_2 , A_3). The other two parameters are the baseflow index (BFI) and the daily recession constant (K), which is used to determine the proportion of baseflow recharge from surface runoff and discharge from the baseflow, respectively. Thus, the parameter vector associated with the AWBM model can be written as $\theta = (C_1, C_2, C_3, A_1, A_2, A_3, \text{BFI}, K)$.

4.2.1. Parameter uncertainty estimation

In this section, we focus to investigate the performances of the SMC samplers in identifying and estimating model parameters without explicit assessment of forcing data error. Here, we considered two different runoff time series in this analysis. The first study serves as a benchmark experiment of the SMC samplers and uses a fourteen years (1 January 1983–31 December 1996) record of simulated dataset. The simulated runoff dataset was generated

from the AWBM model using measured forcing data from the Bass River watershed in the South Gippsland Basin (52 km^2) and parameter values given by Marshall et al. (2004) (Table A1 in **Supplement 3**). The artificial runoff data are then corrupted with heteroscedastic measurement error, the standard deviation of which was taken to vary from 5% to 50% of the actual simulated values. The second study explores the performance of the SMC samplers using the actual measured runoff dataset (see details in Bates and Campbell, 2001; Marshall et al., 2004; Jeremiah et al., 2011). In all numerical experiments, the SMC samplers were performed with particle number $N = 400$ and iteration $S = 1000$, where the initial parameter values were randomly sampled from the noninformative prior distribution (Moradkhani et al., 2005; Salamon and Feyen, 2009).

For the artificial runoff dataset, two main conclusions can be drawn from the analysis. First, the mixing capacity of the RWM-SMC sampler is quite poor (Fig. 6), and it turned out not to be competitive when applying in the hydrologic setting. Second, the ARM-SMC and PEM-SMC samplers are robust to noise in measurements. The estimates of the model parameters derived with the ARM-SMC and PEM-SMC are very close to the actual values when the standard deviation of measurement error varies from 5% to 30% of the actual simulated values (Fig. 7). Previous studies have illustrated that the overall uncertainty in runoff measurements mainly range from 5% to 20% (Pelletier, 1987). Thus, the effect of measurement uncertainty plays a marginal role in identifying real-world hydrological model parameters for the ARM-SMC and PEM-SMC samplers. These highlight that ARM-SMC and PEM-SMC samplers are more suitable than the RWM-SMC sampler in making inferences about the posterior parameter distribution of the hydrological models. In the following study, we thus mainly focus on investigating the performances of the ARM-SMC and PEM-SMC samplers in real-world hydrological setting.

For the historical runoff observations, we used 5 years (1 January 1987–31 December 1991) data for model calibration, and 5 years (1 January 1992–31 December 1996) data for model validation. To reduce sensitivity to state value initialization, the first 4-year data (1 January 1983–31 December 1986) was used as the warm up period prior to the calibration data time series, during which no updating of the posterior density was performed. The

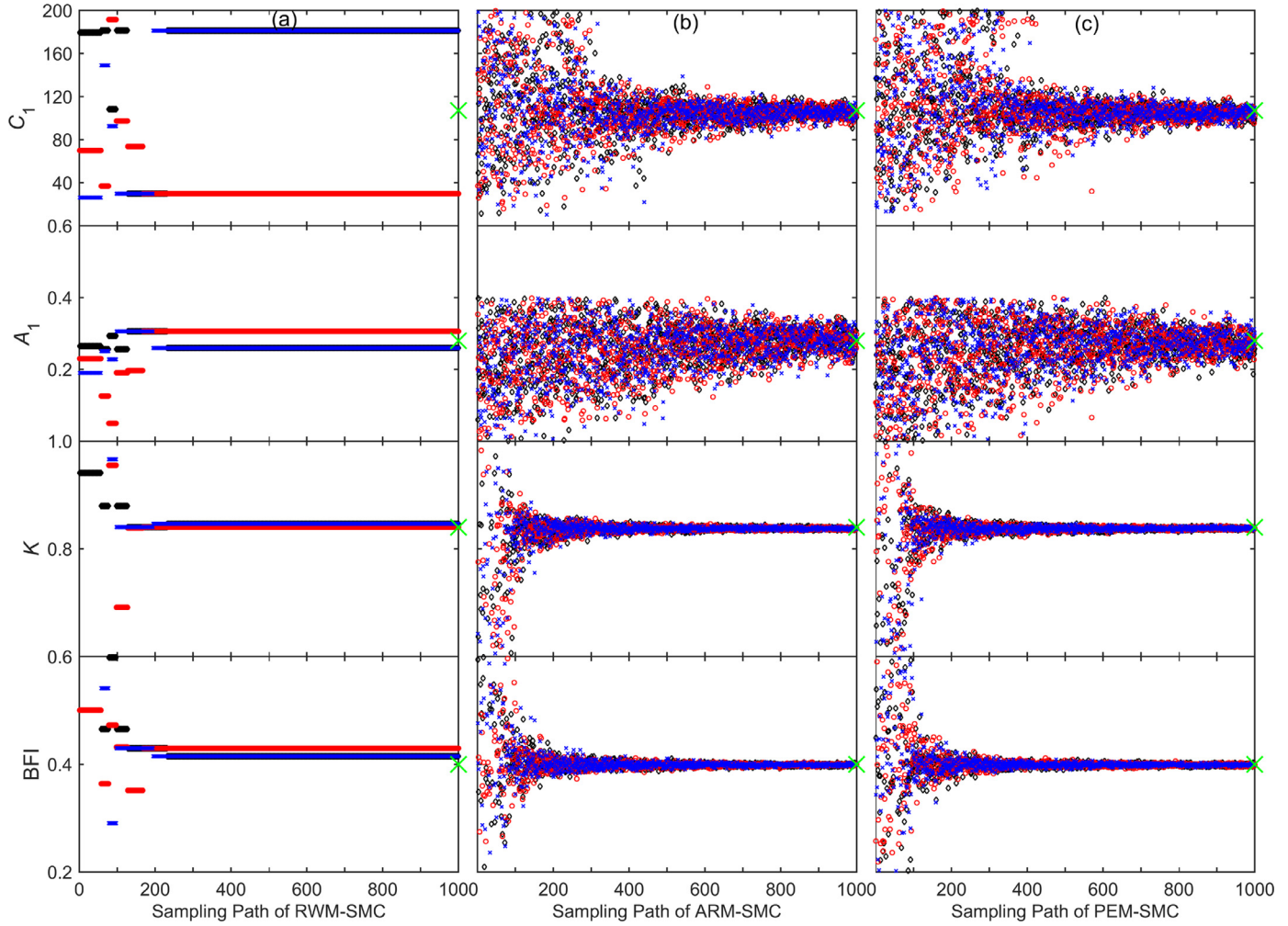


Fig. 6. Transitions of the sampled parameter values in three randomly selected particles during the sampling path using (a) RWM-SMC, (b) ARM-SMC, and (c) PEM-SMC samplers without considering the input errors. The cross symbol at the right hand side indicate the actual parameter values used to generate the synthetic runoff data. Different particle is coded with a different symbol and color.

Table 2

Summary of the posterior marginal parameter distribution for the AWBM using historical runoff dataset with/without considering input uncertainty.

Parameter	Prior Range	Without input uncertainty ARM-SMC			Without input uncertainty PEM-SMC			With input uncertainty ARM-SMC			With input uncertainty PEM-SMC		
		2.5% ^a	median	97.5% ^a	2.5% ^a	median	97.5% ^a	2.5% ^a	median	97.5% ^a	2.5% ^a	median	97.5% ^a
C_1	0–200	19.3	80.4	193.6	20.8	81.7	163.2	57.2	82.5	102.7	86.4	92.5	99.8
C_2	0–300	167.7	235.9	295.6	175.9	221.6	279.2	224.6	245.0	266.9	177.9	186.4	195.9
C_3	0–5000	110.4	236.9	317.6	158.9	263.2	363.2	451.3	512.0	602.8	609.5	632.8	656.7
A_1	0–1.0	0.02	0.15	0.28	0.07	0.16	0.25	0.11	0.14	0.17	0.22	0.23	0.25
A_2	0–1.0	0.17	0.50	0.65	0.30	0.50	0.64	0.18	0.24	0.32	0.22	0.24	0.27
A_3	0–1.0	0.14	0.34	0.66	0.13	0.34	0.62	0.53	0.62	0.68	0.49	0.53	0.55
K	0–1.0	0.80	0.84	0.89	0.82	0.86	0.89	0.94	0.95	0.97	0.91	0.92	0.93
BFI	0–1.0	0.35	0.39	0.43	0.35	0.38	0.43	0.50	0.53	0.54	0.56	0.57	0.58
B	0.25–2.5	N/A	N/A	N/A	N/A	N/A	N/A	0.68	1.36	1.94	0.91	1.35	1.85

^a 2.5% and 97.5% represents the 2.5 and 97.5 percentile of the posterior marginal parameter distribution;

posterior marginal parameter distributions derived by each SMC sampler are shown as histograms in Fig. 8 and summarized in Table 2 by posterior medians and 95% probability intervals. The posterior distributions of the individual parameters obtained by the two samplers are very similar and occupy only a relatively small region interior to the uniform prior distributions (Table 2 and Fig. 8), suggesting the two SMC samplers were in most cases successful in reducing the assumed prior uncertainties of the parameters values.

To understand the influence of parameters uncertainty to the simulation result of AWBM predictive uncertainty, Fig. 9 shows the 95% hydrograph prediction uncertainty intervals associated with the posterior parameters ranges for the selected calibration and evaluation periods. We can observe that the ensemble runoff predictions using the posterior parameters derived by the two SMC samplers are very similar and they all reasonably track the historical runoff dynamics (dark solid circles). However, only a small portion of observed runoff data can be bracketed by the 95% hydrograph prediction uncertainty (Table 3 and Fig. 9). The findings

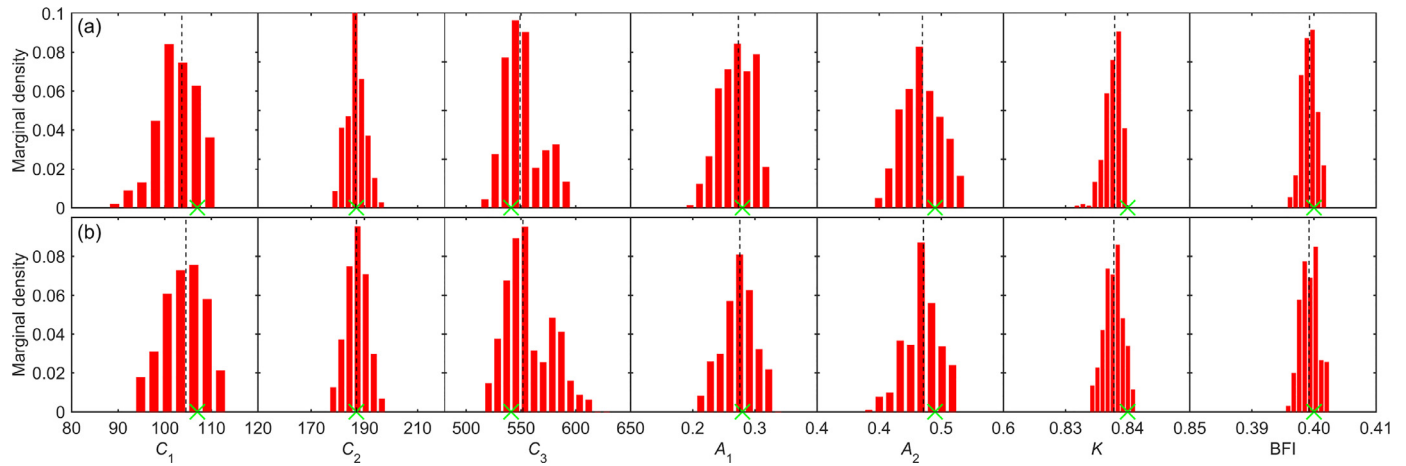


Fig. 7. Histograms of the marginal posterior parameter distributions of the AWBM model derived by (a) ARM-SMC and (b) PEM-SMC samplers at the end of simulation using synthetic runoff dataset without considering the input errors. The cross symbol at the bottom side indicate the actual parameter values used to generate the synthetic runoff data. The dash line indicates the median parameter values estimated by the SMC samplers.

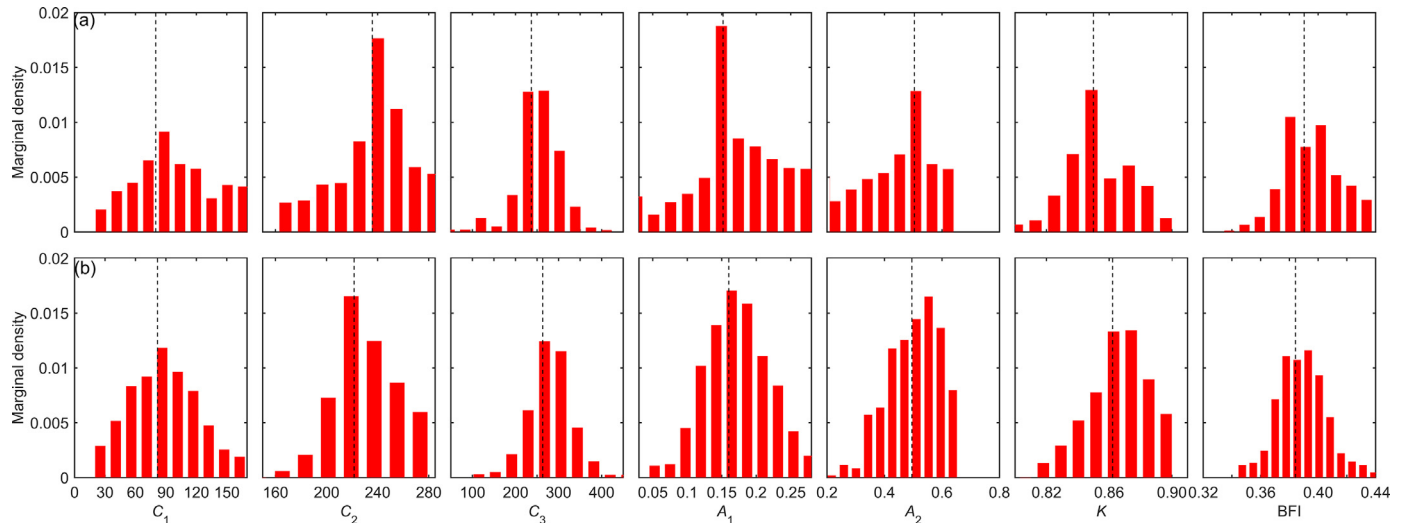


Fig. 8. Histograms of the marginal posterior parameter distributions of the AWBM model derived with (a) ARM-SMC and (b) PEM-SMC samplers at the end of simulation using historical observations without considering the input errors.

Table 3

Statistics of model performances using posterior median parameter values obtained by the two SMC samplers with/without considering input uncertainty.

	Without input uncertainty				With input uncertainty			
	Calibration period		Validation period		Calibration period		Validation period	
	ARM-SMC	PEM-SMC	ARM-SMC	PEM-SMC	ARM-SMC	PEM-SMC	ARM-SMC	PEM-SMC
Slope	0.68	0.70	1.14	1.13	0.73	0.76	0.82	0.84
R ²	0.69	0.70	0.66	0.66	0.71	0.73	0.68	0.70
RMSE	7.39	7.39	5.95	5.89	6.99	6.18	4.29	4.16
Bias	1.02	1.03	0.88	0.83	-0.38	-0.23	0.15	0.07
Bracketing Percentage	14.4	13.8	14.2	12.9	22.9	20.5	21.2	20.8

Slope: the slope of regression line between the observed and simulated runoff; R²: the coefficient of determination; RMSE: root-mean-square error; Bias: mean bias between the observed and simulated runoff; Bracketing Percentage: the percentage of observations fall in the 95% predication uncertainty bounds.

are consistent with previous studies (i.e., Ajami et al., 2007; Vrugt et al., 2008), and reveal a considerable amount of uncertainty in both the model structure and the forcing data.

4.2.2. Simultaneously considering parameter and input uncertainty estimation

In this section, we investigate the applicability of the SMC samplers in simultaneous estimation of the AWBM model parameters and input uncertainty within the system. In this study, the rain-

fall forcing data error was implemented by using a single rainfall multiplier for each storm event (Kavetski et al., 2002, 2006; Ajami et al., 2007; Vrugt et al., 2008). That is, each storm is assigned a different rainfall multiplier β_j ($j = 1, 2, \dots, \varsigma$) which uniformly distributed over the range between 0.25 and 2.50, and these values are added to the vector of model parameters θ to be optimized; hence $\theta = [\theta; \beta]$. In the 5 years calibration period (1 January 1987–31 December 1991), a total of $\varsigma = 66$ storm events were identified for the Bass River watershed, which resulted in the number

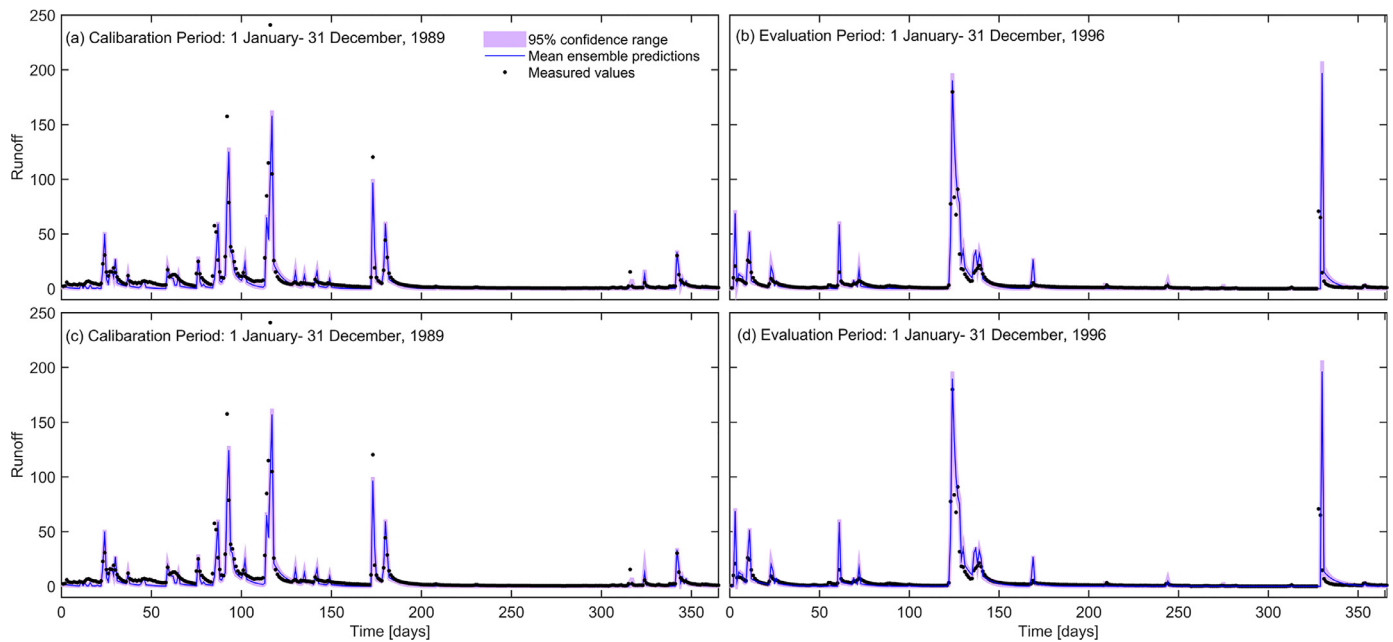


Fig. 9. Comparison of observed (dots) and 95% hydrograph prediction uncertainty intervals (dark gray region) by (a) ARM-SMC and (c) PEM-SMC during selected calibration period, and (b) ARM-SMC and (d) PEM-SMC during selected evaluation period when only considering parameter uncertainty.

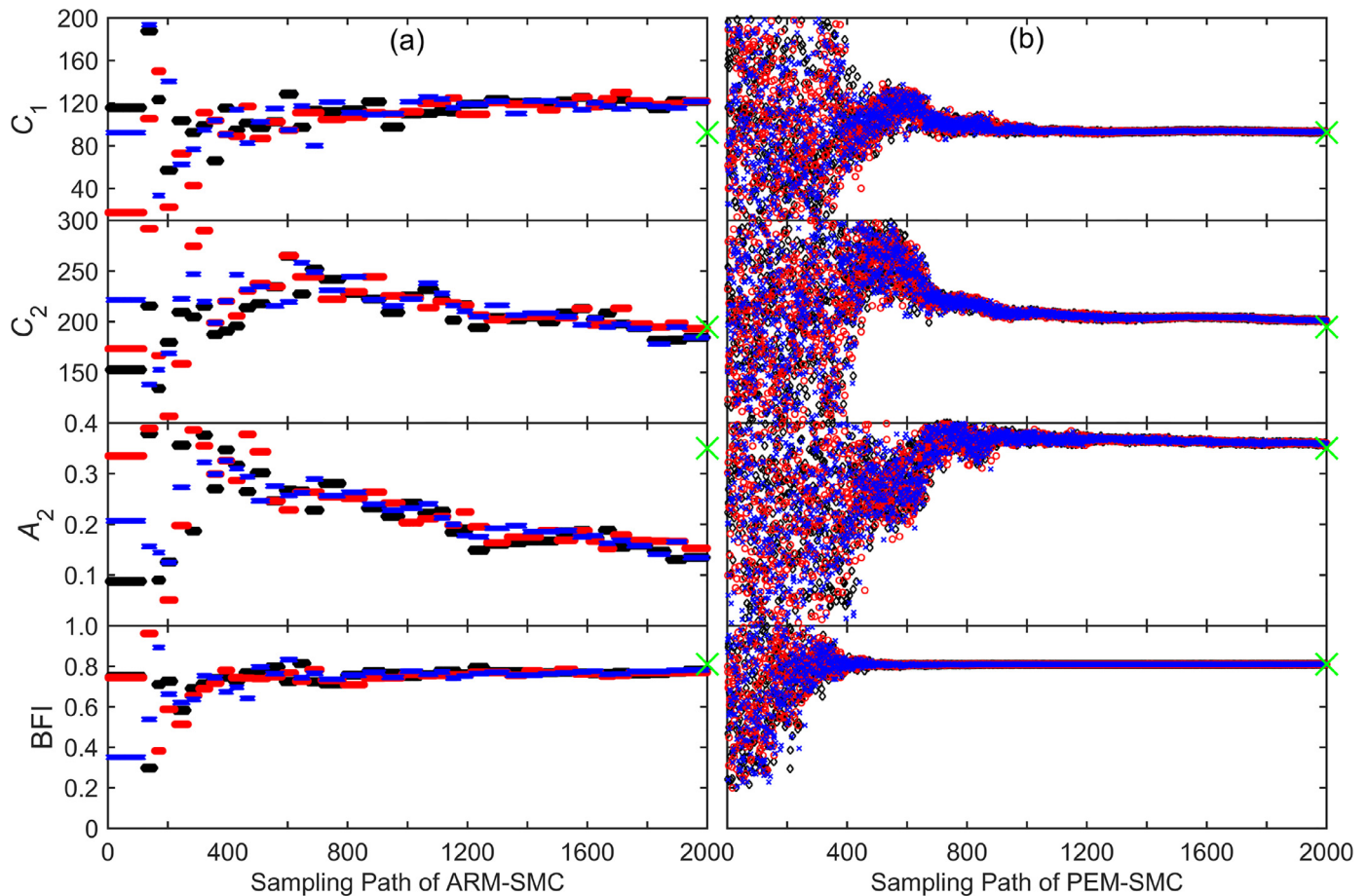


Fig. 10. Transitions of the sampled model parameter values in three randomly selected particles during the sampling path using (a) ARM-SMC and (b) PEM-SMC samplers when accounting for the input errors. The cross symbol at the right hand side indicate the actual parameter values used to generate the synthetic runoff data. Different particle is coded with a different symbol and color.

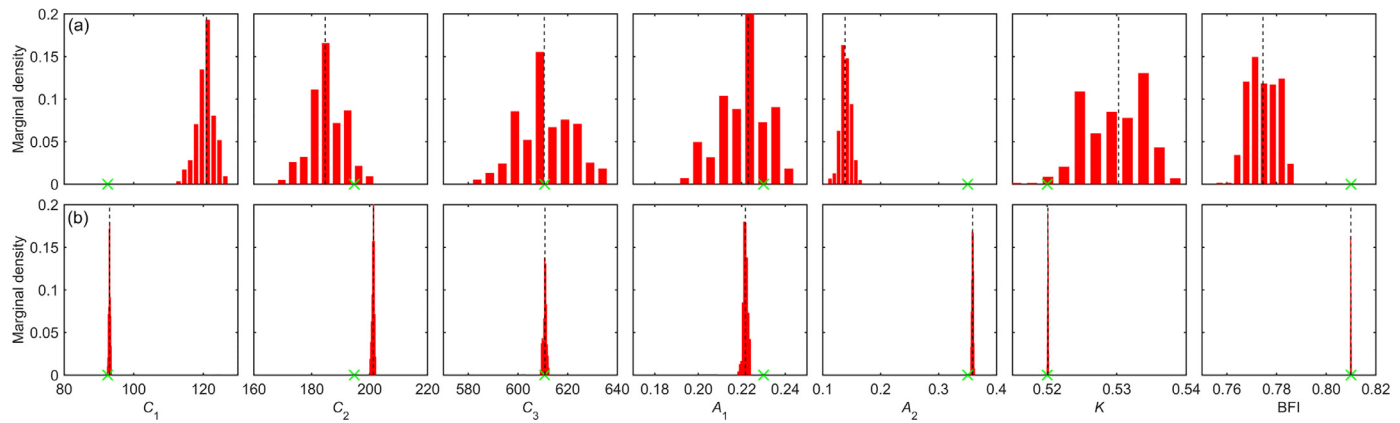


Fig. 11. Histograms of the marginal posterior parameter distributions of the AWBM model derived with (a) ARM-SMC and (b) PEM-SMC samplers at the end of simulation when accounting for the input errors. The cross symbol at the bottom side indicate the actual parameter values used to generate the synthetic runoff data. The dash line indicates the median parameter values estimated by the SMC samplers.

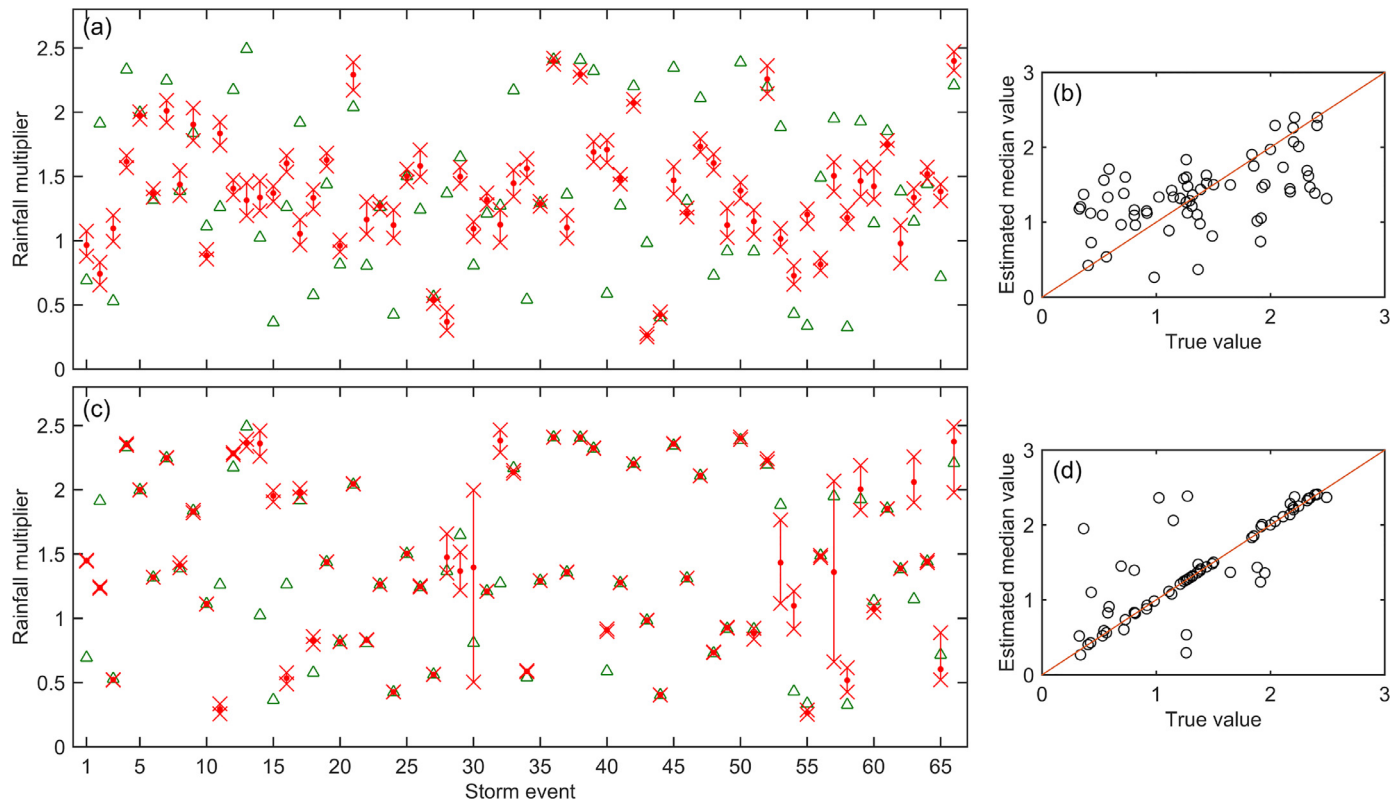


Fig. 12. Posterior median estimates (closed circles) and 95% probability intervals (cross) for the rainfall multipliers obtained by the (a) ARM-SMC sampler and (c) PEM-SMC sampler. The triangle indicates the actual rainfall multiplier values used to generate the synthetic runoff data. (b) and (d) showed the regression between the estimated median and actual values of the rainfall multipliers for the ARM- and PEM-SMC, respectively.

of estimated parameters increasing up to 73. To verify whether the SMC samplers are computationally feasible, synthetically generated runoff data are used first, followed by the actual measured runoff dataset. To generate the synthetic runoff dataset, a multiplier vector was first drawn using Latin hypercube sampling within $[0.25, 2.50]^S$ ($S=66$). Then, it was combined with the observed rainfall depths over the basin to generate a new rainfall hyetograph. The rainfall record was subsequently used with randomly sampled values of the AWBM parameters (Table A2 in **Supplement 3**) to create a 5-year time series of synthetic runoff data. In both the synthetic and the actual studies, the SMC samplers were performed with particle number $N=600$ and iteration $S=2000$.

For the synthetic runoff dataset, it is observed that the particles generated by the SMC samplers tend to converge to the limiting distribution after 1200 iterations (Fig. 10). However, the ARM-SMC sampler provides some differing parameter estimates from their actual values, in particular for parameters C_1 , C_2 and A_2 , while the different actual values of the AWBM model parameters are well defined by the PEM-SMC sampler and display very little uncertainty (Fig. 11). More significantly, it is difficult for the ARM-SMC sampler to properly converge to the actual values of the rainfall multipliers (only 11 out of 66 are well identified). On the contrary, the majority of the rainfall multiplier values (41 out of 66) are well identified by the PEM-SMC sampler with its failures due to the low values in either rainfall depths or runoff observations (Fig. 12).

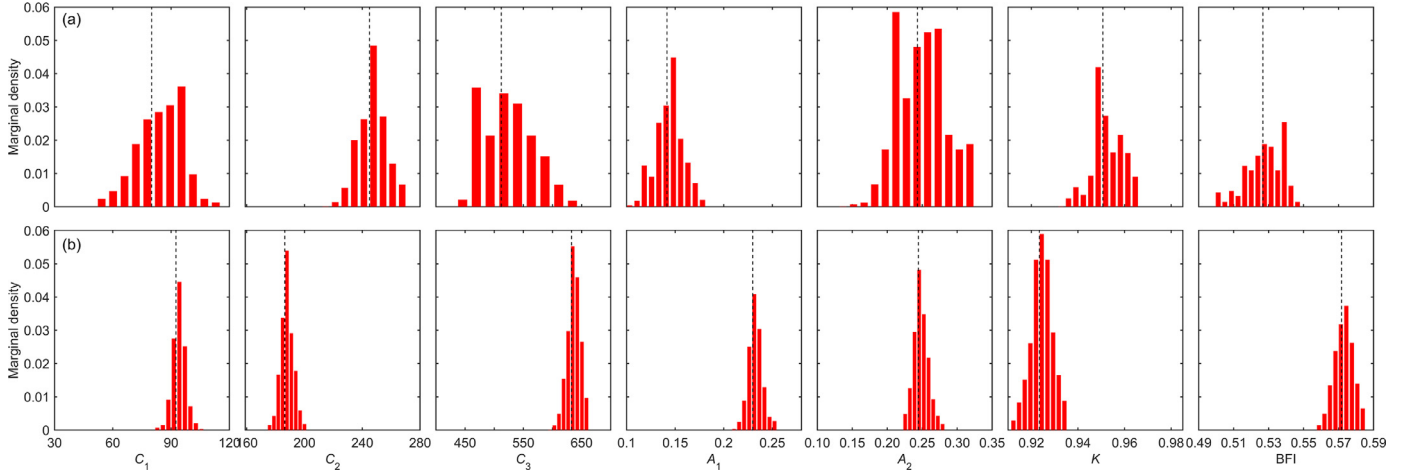


Fig. 13. Histograms of the marginal posterior parameter distributions of the AWBM model derived with (a) ARM-SMC and (b) PEM-SMC samplers at the end of simulation using historical observations when accounting for the input errors.

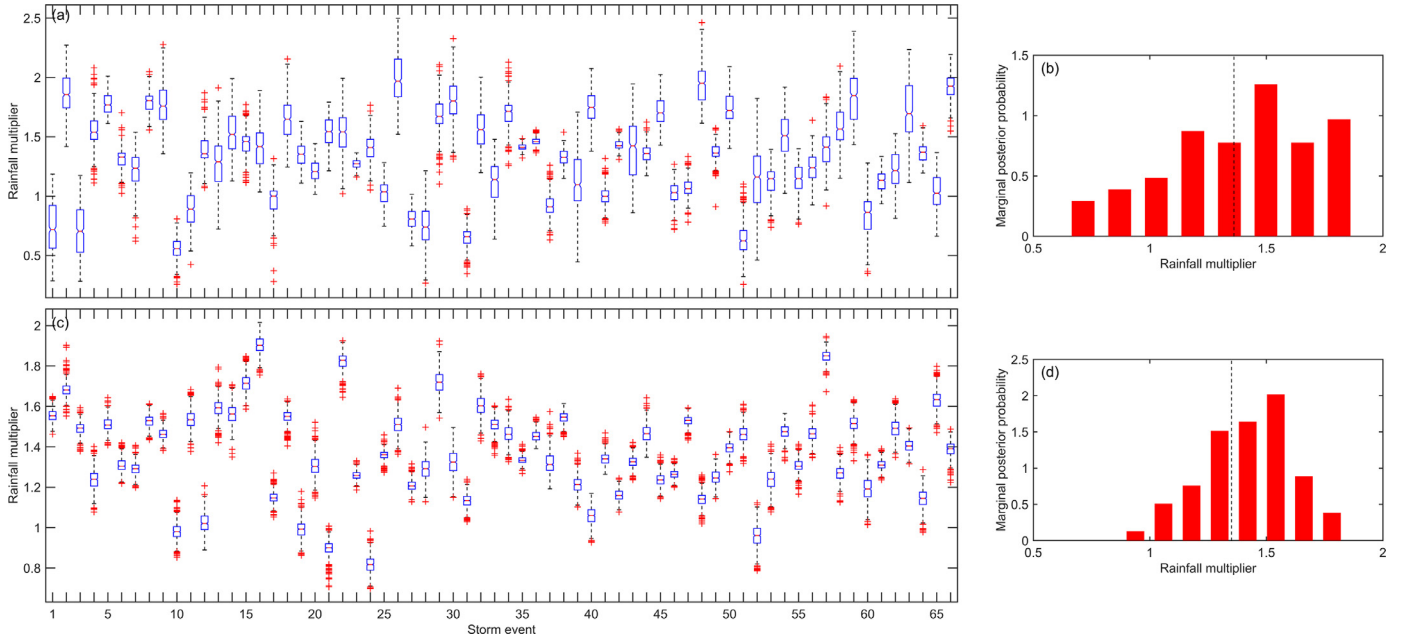


Fig. 14. Box plots of the marginal posterior distributions of the rainfall multipliers for each storm event obtained by (a) ARM-SMC and (c) PEM-SMC. Histograms of all combined storm multipliers estimated by (b) ARM-SMC and (d) PEM-SMC.

Thus, the PEM-SMC sampler is more robust than the ARM-SMC sampler for the case in simultaneously estimating both the AWBM model parameters and the rainfall multipliers. More details about the performances of the SMC samplers were presented in **Supplement 3**.

For the historical runoff observations, the calibration procedure is similar to that used in [Section 4.2.1](#). The posterior marginal parameter distributions derived by the SMC samplers are given in [Fig. 13](#) and [Table 2](#). The sampled rainfall multipliers for each storm are presented as box plots in [Fig. 14](#), as well as providing histograms of all combined rainfall multipliers. Comparing with the results in [Section 4.2.1](#), we can observe that: (1) the explicit consideration of the input error changes the final estimated marginal distribution of the model parameters, which is most evident for the parameters C_3 , K and BFI ([Table 2](#)); (2) the 95% prediction uncertainty interval of the parameters obtained by the SMC samplers decreases when rainfall estimates are directly inferred from the observed discharge data ([Table 2](#)); (3) the posterior distribution of the model parameters and the rainfall multipliers derived

by the PEM-SMC sampler are very narrow and close to normal in comparison with that obtained by the ARM-SMC sampler ([Fig. 13](#); [Fig. 14a](#) and [c](#)), indicating that the runoff observations contain sufficient information for the PEM-SMC sampler to simultaneously constrain both model parameters and rainfall multipliers; and (4) the median posterior values of the combined rainfall multipliers obtained by the two SMC samplers are very similar and larger than 1 ([Fig. 14b](#) and [d](#)), indicating the observed rainfall depths are lower than our inferred rainfall from the runoff data on average.

The 95% runoff predictive uncertainty ranges associated with model parameter and input uncertainty for selected calibration and evaluation periods are presented in [Fig. 15](#). Here, the rainfall multiplier for each individual rainfall storm during the evaluation period was sampled from the histograms presented in [Fig. 14b](#) and [d](#), and was then combined with the observed rainfall record to generate a possible realization of rainfall hyetograph. Looking at [Fig. 15](#) and comparing with [Fig. 9](#), we can observe that the 95% prediction intervals are slightly narrow here and show a much better coverage

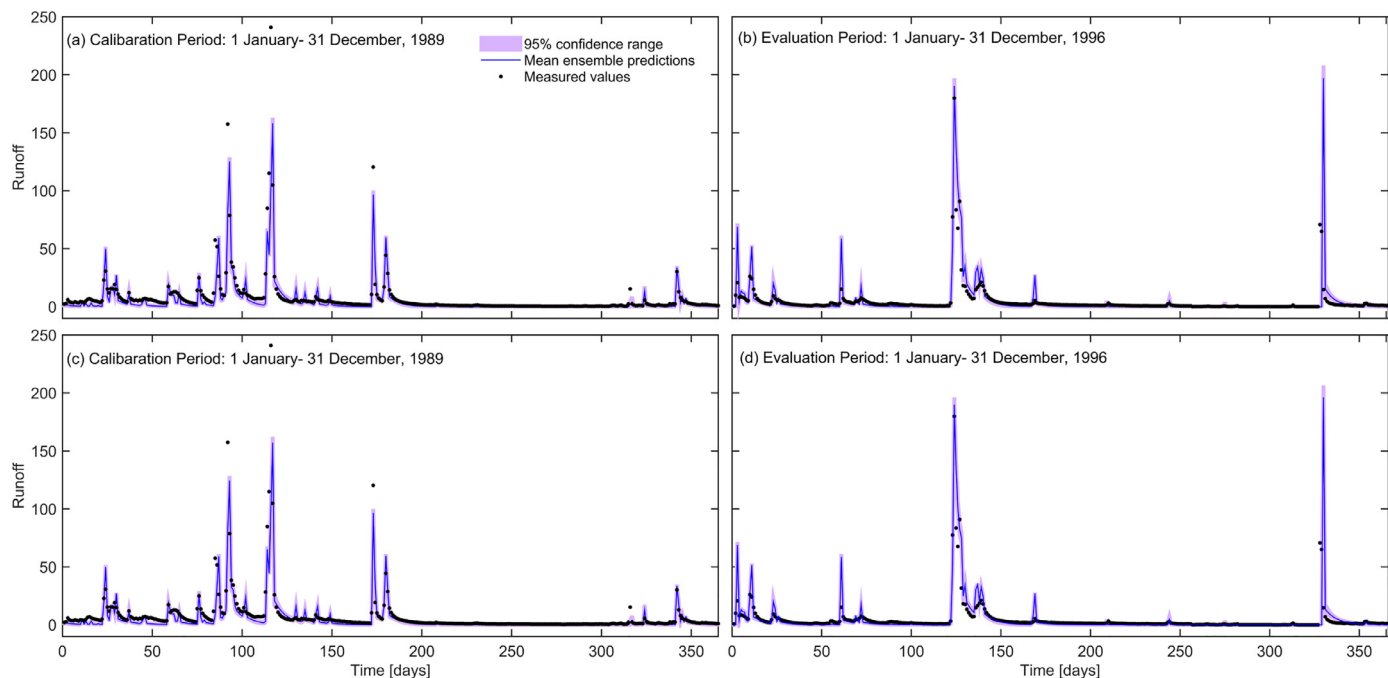


Fig. 15. Comparison of observed (dots) and 95% hydrograph prediction uncertainty intervals (dark gray region) by (a) ARM-SMC and (c) PEM-SMC during selected calibration period, and (b) ARM-SMC and (d) PEM-SMC during selected evaluation period when accounting for the input errors.

of the low runoff observations (i.e., days 1–81 for calibration period and days 1–50 for the validation period). The summary statistics presented in Table 3 showed that the observed runoff data that fall in the 95% prediction intervals has increased by about 50% for the two SMC samplers when we account for input uncertainty. Also, a better model performance is obtained when rainfall multipliers are simultaneously inferred with the model parameters (i.e., a 5%–30% reduction in RMSE is observed for the two SMC samplers). Noticeably, the model performances with parameters and input uncertainty determined by the AWR-SMC sampler and the PEM-SMC sampler are very similar. This phenomenon is well known as “equifinality” in hydrology mainly due to the inadequacies in model structure (Beven and Freer, 2001; Bastola et al., 2011). Thus, further analysis about model structural error is needed in future studies. This is beyond the scope of current paper, and we will consider using multiple different hydrological models to reduce the uncertainty caused by the model structure in future studies.

5. Conclusions

This paper has presented a sequential Monte Carlo sampler, which is entitled the Particle Evolution Metropolis Sequential Monte Carlo (PEM-SMC) algorithm. The sampler incorporates some attractive features of genetic algorithm, differential evolution algorithm and Metropolis-Hastings algorithm into the framework of sequential Monte Carlo to evolve a population of particles to approximate the posterior parameter distributions. We proved that the sampler admits the target distribution at each iteration ($\pi_s(\theta), s=1, 2, \dots, S$) to be a stationary distribution. The performance of the PEM-SMC in estimating the posterior parameter distribution was compared with the other two SMC samplers (i.e., RWM-SMC, and ARM-SMC samplers) through two case studies of increasing complexity.

The first case study, a synthetic bimodal normal distribution showed that the PEM-SMC sampler has the ability to infer the known target distribution where the parameter surface is extremely complex with many local optima. For the ARM-SMC sam-

pler, the candidates are drawn from the Gaussian proposal distribution with a fixed spatial orientation. Thus, the ARM-SMC sampler is more likely to falsely converge to a local optimum, and only one mode can be identified in dimension $d=20$ (Fig. 3b). This indicated that the ARM-SMC sampler can potentially experience difficulties in exploring the non-Gaussian parameter space with multiple modes. In addition, the difficulty in ensuring the weighted sample covariance matrix to be symmetric and positively semi-defined make the ARM-SMC sampler thoroughly fails for high dimensional problems ($d=30$). For the RWM-SMC, the candidates are generated from an isotropic random walk, which can effectively reduce the risk of false convergence to local optima. However, the RWM-SMC algorithm shows relative poor mixing property, and it is generally difficult for the individual particles to traverse the parameter space (Figs. 1 and 3). This leads the explorative capability of the RWM-SMC sampler through the feasible parameter space is lower than that of the ARM-SMC and PEM-SMC samplers.

A second case study illustrated the utility of the PEM-SMC sampler when applied to conceptual rainfall-runoff modeling by only considering model parameter uncertainty and simultaneously considering both model parameter and input data uncertainties. The synthetic test reveals that the improved efficiency and effectiveness of the PEM-SMC sampler can successfully reduce the prior uncertainties in parameter and input by using information contained in observed runoff data (Jeremiah et al., 2011). On the contrary, the RWM-SMC sampler turned out to not competitive when applying in the hydrologic setting due to its low capacity in exploring parameter space. This is consistent with the results of the synthetic bimodal normal distribution. The ARM-SMC sampler experienced difficulties in simultaneously estimating both the model parameters and the input uncertainties. The majority of the actual values of the rainfall multipliers fall out the 95% probability intervals obtained by the ARM-SMC sampler (Fig. 12). For historical runoff observations, the estimated marginal distribution of the model parameters by accounting input errors was different from that estimated by only considering parameter uncertainty (Table 2). In addition, the observed runoff data that fall in the

95% prediction intervals has increased by about 50% for the two SMC samplers when we account for input errors (Table 3). These results are consistent with previous studies (Ajmi et al., 2007; Vrugt et al., 2008). However, the model performances with different parameter and rainfall multiplier values determined by the ARW-SMC and PEM-SMC samplers are very similar. This indicates that some physical processes of the watershed may be not adequately represented by the AWBM model, and further analysis is needed to address the model structure uncertainty by using the Bayesian model averaging approach (Ajmi et al., 2007; Qi et al., 2018), the integration of copulas and Bayesian model averaging approach (Madadgar & Moradkhani, 2013; Madadgar et al., 2014), sequential Bayesian methods (Hsu et al., 2009; Wei et al., 2012) and data assimilation methods (Bell et al., 2004; Kuppel et al., 2013; Cardinali et al., 2014; Abbaszadeh et al., 2018). Essentially, Bayesian model averaging approach is a post-processing of the individual model predictions in a selected ensemble by using the Expectation–Maximization (EM) algorithm (Raftery et al., 1997). Thus, the proposed SMC sampler can be easily extended to the studies of total uncertainty assessment including model parameters, input and structural uncertainty, and we will present related results in the coming papers. Finally, the computational execution time required by the PEM-SMC sampler is about two times of that needed by the RWM-SMC and ARM-SMC samplers because of the inclusion of some extra operators in move step of the PEM-SMC sampler. However, a further significant speedup can be obtained if the PEM-SMC is executed on a parallel machine or a network of computers due to its inherently parallel. This is especially true for real-world hydrological problems where obtaining the proper parameter posterior distributions often requires a significant amount of time (i.e., about 20 hours for simultaneously estimating both parameter and input uncertainties of the AWBM model for the PEM-SMC sampler).

Acknowledgments

The authors would thank Prof. G.C. Sander (Editor) and Prof. B. Rajagopalan (Associate Editor) for their continued help during the revisions of the paper. We also thank the anonymous reviews for their critical reviews and helpful comments. This research was supported by National Key R & D Program of China(2016YFC0500203), the National Natural Science Foundation of China (Nos. 31370467 and 41571016), and CAS Interdisciplinary Innovation Team. The data and code written in MATLAB can be obtained from the first author (zhugf@lzu.edu.cn) upon request.

Supplementary materials

Supplementary material associated with this article can be found, in the online version, at doi:[10.1016/j.advwatres.2018.02.007](https://doi.org/10.1016/j.advwatres.2018.02.007).

References

- Abbaszadeh, P., Moradkhani, H., Yan, H., 2018. Enhancing hydrologic data assimilation by evolutionary particle filter and Markov Chain Monte Carlo. *Adv. Water Resour.* 111, 192–204.
- Ajami, N.K., Duan, Q., Sorooshian, S., 2007. An integrated hydrologic Bayesian multi-model combination framework: confronting input, parameter, and model structural uncertainty in hydrologic prediction. *Water Resour. Res.* 43, W01403. <https://doi.org/10.1029/2005WR004745>.
- Arulampalam, M.S., Maskell, S., Gordon, N., Clapp, T., 2002. A tutorial on particle filters for online nonlinear/non Gaussian Bayesian tracking. *IEEE Trans. Signal Process.* 50 (2), 174–188. <https://doi.org/10.1109/78.978374>.
- Bastola, S., Murphy, C., Sweeney, J., 2011. The role of hydrological modelling uncertainties in climate change impact assessments of Irish river catchments. *Adv. Water Resour.* 34, 562–576.
- Bates, B.C., Campbell, E.P., 2001. A Markov chain Monte Carlo scheme for parameter estimation and inference in conceptual rainfall-runoff modeling. *Water Resour. Res.* 37 (4), 937–947.
- Bell, M.J., Martin, M.J., Nichols, N.K., 2004. Assimilation of data into an ocean model with systematic errors near the equator. *Q. J. R. Meteorol. Soc.* 130, 873–893.
- Beven, K., Freer, J., 2001. Equifinality, data assimilation, and data uncertainty estimation in mechanistic modelling of complex environmental systems using the GLUE methodology. *J. Hydrol.* 249, 11–29.
- Boughton, W.C., 1993. A hydrograph-based model for estimating the water yield of ungauged catchments. In: *Nat. Conf. Publ. Inst. Eng. Aust.*, 93, pp. 317–324.
- Braswell, B., Sacks, W.J., Linder, E., Schimel, D.S., 2005. Estimating diurnal to annual ecosystem parameters by synthesis of a carbon flux model with eddy covariance net ecosystem exchange observations. *Global Change Biol* 11, 1–21.
- Cardinali, C., Zagar, N., Radnoti, G., Buizza, R., 2014. Representing model error in ensemble data assimilation. *Nonlin. Processes Geophys.* 21, 971–985.
- Chopin, N., 2002. A sequential particle filter method for static models. *Biometrika* 89 (3), 539–552.
- Clark, J.S., 2005. Why environmental scientists are becoming Bayesians. *Ecol. Lett.* 8, 2–14.
- Clark, M.P., Nijssen, B., Lundquist, J.D., Kavetski, D., Rupp, D.E., Woods, R.A., Freer, J.E., Gutmann, E.D., Wood, A.W., Brekke, L.D., Arnold, J.R., Gochis, D.J., Rasmussen, R.M., 2015. A unified approach for process-based hydrologic modeling: 1. modeling concept. *Water Resour. Res.* 51 (4), 2498–2514. <https://doi.org/10.1002/2015WR017198>.
- Del Moral, P., Doucet, A., Jasra, A., 2006. Sequential Monte Carlo samplers. *J. R. Stat. Soc., Ser. B* 68, 411–436.
- Duan, Q., Sorooshian, S., Gupta, V., 1992. Effective and efficient global optimization for conceptual rainfall-runoff models. *Water Resour. Res.* 28 (4), 1015–1031.
- Fan, Y., Leslie, D.S., Wand, M.P., 2008. Generalised linear mixed model analysis via sequential Monte Carlo sampling. *Electron. J. Stat.* 2, 916–938.
- Gao, M., Zhang, H., 2012. Sequential Monte Carlo methods for parameter estimation in nonlinear state-space models. *Comput. Geosci.* 44, 70–77.
- Gelman, A.B., Carlin, J.S., Stern, H.S., Rubin, D.B., 1995. In: Chatfield, C., Zidek, J.V. (Eds.), *Bayesian Data Analysis*, Texts in Stat. Sci. Ser.. CRC Press, Boca Raton, Florida.
- Gupta, H.V., Sorooshian, S., Yapo, P.O., 1998. Toward improved calibration of hydrologic models: multiple and noncommensurable measures of information. *Water Resour. Res.* 34 (4), 751–763.
- Holland, J.H., 1975. *Adaptation in Natural and Artificial Systems*. University of Michigan Press, Ann Arbor.
- Hsu, K.-L., Moradkhani, H., Sorooshian, S., 2009. A sequential Bayesian approach for hydrologic model selection and prediction. *Water Resour. Res.* 45, W00B12. <https://doi.org/10.1029/2008WR006824>.
- Jeremiah, E., Sisson, S., Sharma, A., Marshall, L., 2012. Efficient hydrological model parameter optimization with Sequential Monte Carlo sampling. *Environ. Modell. Software* 38, 283–295.
- Jeremiah, E., Sisson, S., Marshall, L., Mehrotra, R., Sharma, A., 2011. Bayesian calibration and uncertainty analysis of hydrological models: A comparison of adaptive Metropolis and sequential Monte Carlo samplers. *Water Resour. Res.* 47, W07547. <https://doi.org/10.1029/2010WR010217>.
- Kavetski, D., Kuczera, G., Franks, S.W., 2006. Bayesian analysis of input uncertainty in hydrological modeling: 2. Application. *Water Resour. Res.* 42, W03408. <https://doi.org/10.1029/2005WR004376>.
- Kavetski, D., Franks, S.W., Kuczera, G., et al., 2002. Confronting input uncertainty in environmental modeling. In: Duan, Q., et al. (Eds.). In: *Calibration of Watershed Models*. Water Sci. Appl., 6. AGU, Washington, D.C, pp. 49–68.
- Kuppel, S., Chevallier, F., Peylin, P., 2013. Quantifying the model structural error in carbon cycle data assimilation systems. *Geosci. Model Dev.* 6, 45–55.
- Lee, D.S., Chia, N.K.K., 2002. A particle algorithm for sequential Bayesian parameter estimation and model selection. *IEEE Trans. Signal Process.* 50 (2), 326–336.
- Li, M., Pang, B., He, Y., F. Nian, 2013. particle filter improved by genetic algorithm and particle swarm optimization algorithm. *J. Softw.* 8 (3), 666–672.
- Liang, F.M., Wong, W.H., 2001. Real-parameter evolutionary Monte Carlo with applications to Bayesian mixture models. *J. Am. Stat. Assoc.* 96, 653–666.
- Madadgar, S., Moradkhani, H., 2013. Drought analysis under climate change using Copula. *J. Hydrol. Eng.* 18 (7), 746–759.
- Madadgar, S., Moradkhani, H., Garen, D., 2014. Towards improved post-processing of hydrologic forecast ensembles. *Hydro. Processes* 28, 104–122.
- Marshall, L., Nott, D., Sharma, A., 2004. A comparative study of Markov chain Monte Carlo methods for conceptual rainfall-runoff modeling. *Water Resour. Res.* 40, W02501. <https://doi.org/10.1029/2003WR002378>.
- Mendoza, P.A., Clark, M.P., Barlage, M., Rajagopalan, B., Samaniego, L., Abramowitz, G., Gupta, H., 2015. Are we unnecessarily constraining the agility of complex process-based models? *Water Resour. Res.* 51, 716–728. <https://doi.org/10.1002/2014WR015820>.
- Metropolis, N., Rosenbluth, A.W., Rosenbluth, M.N., Teller, A.H., Teller, E., 1953. Equation of state calculations by fast computing machines. *J. Chem. Phys.* 21, 1087–1092.
- Montanari, A., 2005. Large sample behaviors of the generalized likelihood uncertainty estimation (GLUE) in assessing the uncertainty of rainfall-runoff simulations. *Water Resour. Res.* 41, W08406. <https://doi.org/10.1029/2004WR003826>.
- Montanari, A., 2007. What do we mean by ‘uncertainty’? The need for a consistent wording about uncertainty assessment in hydrology. *Hydrol. Process.* 21, 841–845.
- Montanari, A., Koutsoyiannis, D., 2012. A blueprint for process-based modeling of

- uncertain hydrological systems. *Water Resour. Res.* 48, W09555. <https://doi.org/10.1029/2011WR011412>.
- Moradkhani, H., DeChant, C.M., Sorooshian, S., 2012. Evolution of ensemble data assimilation for uncertainty quantification using the particle filter Markov Chain Monte Carlo Chain Monte Carlo Method. *Water Resour. Res.* 48, W12520. <https://doi.org/10.1029/2012WR012144>.
- Moradkhani, H., Hsu, K., Gupta, H., Sorooshian, S., 2005. Uncertainty assessment of hydrologic model states and parameters: sequential data assimilation using the particle filter. *Water Resour. Res.* 41, W05012. <https://doi.org/10.1029/2004WR003604>.
- Nagarajan, K., Judge, J., Graham, W.D., Monsivais-Huerto, A., 2011. Particle filter-based assimilation algorithms for improved estimation of root-zone soil moisture under dynamic vegetation conditions. *Adv. Water Resour.* 34 (4), 433–447.
- Noh, S.J., Tachikawa, Y., Shiiba, M., Kim, S., 2011. Applying sequential Monte Carlo methods into a distributed hydrologic model: lagged particle filtering approach with regularization. *Hydrol. Earth Syst. Sci.* 15, 3237–3251.
- Owen, A.B., Tribble, S.D., 2005. A quasi-Monte Carlo metropolis algorithm. *Proc. Natl. Acad. Sci. U.S.A.* 102, 8844–8849.
- Park, S., Hwang, J., Rou, K., Kim, E., 2007. A new particle filter inspired by biological evolution: genetic filter. In: Proceeding of World Academy of Science, Engineering and Technology, 21, pp. 57–71.
- Pelletier, M.P., 1987. Uncertainties in the determination of river discharge: a literature review. *Can. J. Civ. Eng.* 15, 834–850.
- Pokhrel, P., Gupta, H.V., Wagener, T., 2008. A spatial regularization approach to parameter estimation for a distributed watershed model. *Water Resour. Res.* 44, W12419. <https://doi.org/10.1029/2007WR006615>.
- Pokhrel, P., Yilmaz, K.K., Gupta, H.V., 2012. Multiple-criteria calibration of a distributed watershed model using spatial regularization and response signatures. *J. Hydrol.* 418–419, 49–60.
- Qi, W., Liu, J.G., Yang, H., Sweetapple, C., 2018. An ensemble-based dynamic Bayesian averaging approach for discharge simulations using multiple global precipitation products and hydrological models. *J. Hydrol.* 558, 405–420.
- Raftery, A.E., Madigan, D., Hoeting, J.A., 1997. Bayesian model averaging for linear regression models. *J. Am. Stat. Assoc.* 92, 179–191.
- Roberts, G.O., Rosenthal, J.S., 1998. Markov chain Monte Carlo: some practical implications of theoretical results. *Can. J. Stat.* 26, 5–31.
- Salamon, P., Feyen, L., 2009. Assessing parameter, precipitation, and predictive uncertainty in a distributed hydrological model using sequential data assimilation with the particle filter. *J. Hydrol.* 376, 428–442.
- Smith, T.J., Marshall, L.A., 2008. Bayesian methods in hydrologic modeling: A study of recent advancements in Markov chain Monte Carlo techniques. *Water Resour. Res.* 44, W00B05. <https://doi.org/10.1029/2007WR006705>.
- Storn, R., Price, K., 1997. Differential evolution—a simple and efficient heuristic for global optimization over continuous spaces. *J. Global Optim.* 11, 341–359.
- ter Braak, C.J.F., 2006. A Markov chain Monte Carlo version of the genetic algorithm differential evolution: easy Bayesian computing for real parameter spaces. *Stat. Comput.* 16 (3), 239–249.
- Thiemann, M., Trosset, M., Gupta, H., Sorooshian, S., 2001. Bayesian recursive parameter estimation for hydrological models. *Water Resour. Res.* 37 (10), 2521–2535.
- Uosaki, K., Kimura, Y., Hatanaka, T., 2004. Nonlinear state estimation by evolution strategies based particle filters. In: Proc. Congress on Evolutionary Computation, 1, pp. 884–890.
- Vrugt, J.A., ter Braak, C.J.F., Diks, C.G.H., Schoups, G., 2013. Hydrologic data assimilation using particle Markov chain Monte Carlo simulation: theory, concepts and applications. *Adv. Water Resour.* 51, 457–478.
- Vrugt, J.A., ter Braak, C.J.F., Diks, C.G.H., Higdon, D., Robinson, B.A., Hyman, J.M., 2009. Accelerating Markov chain Monte Carlo simulation by differential evolution with self-adaptive randomized subspace sampling. *Int. J. Nonlinear Sci. Numer. Simul.* 10 (3), 273–290.
- Vrugt, J.A., 2016. Markov chain Monte Carlo simulation using the DREAM software package: theory, concepts, and MATLAB implementation. *Environ. Model. Softw.* 75, 273–316.
- Vrugt, J.A., ter Braak, C.J.F., Clark, M.P., Hyman, J.M., Robinson, B.A., 2008. Treatment of input uncertainty in hydrologic modeling: doing hydrology backward with Markov chain Monte Carlo simulation. *Water Resour. Res.* 44, W00B09. <https://doi.org/10.1029/2007WR006720>.
- Wei, W., Clark, J.S., VOSE, J.M., 2012. Application of a full hierarchical Bayesian model in assessing streamflow response to a climate change scenario at the Coweeta Basin, NC, USA. *J. Resour. Ecol.* 3 (2), 118–128.
- Zhu, G.F., Li, X., Su, Y.H., Zhang, K., Bai, Y., Ma, J.Z., Li, C.B., Hu, X.L., He, J.H., 2014. Simultaneous parameterization of the two-source evapotranspiration model by Bayesian approach: application to spring maize in an arid region of northwest China. *Geosci. Model Dev.* 7, 1467–1482.